Auditory confounds can drive online effects of transcranial ultrasonic stimulation in humans

Benjamin R. Kop[*1], Yazan Shamli Oghli[#2], Talyta C. Grippe[#2], Tulika Nandi[#3], Judith Lefkes[1], Sjoerd W. Meijer[1], Soha Farboud[1], Marwan Engels[1], Michelle Hamani[2], Melissa Null[3], Angela Radetz[3], Umair Hassan[3], Ghazaleh Darmani[2], Andrey Chetverikov[1], Hanneke E.M. den Ouden[†1], Til Ole Bergmann[†3,4], Robert Chen[†2], Lennart Verhagen[1].

*Corresponding author
[#]Equal contribution
[†]Equal senior contribution
[1]Donders Institute for Brain, Cognition, and Behaviour; Radboud University Nijmegen, the Netherlands
[2]Krembil Research Institute, University Health Network; University of Toronto, Canada
[3]Neuroimaging Center; Johannes-Gutenberg University Medical Center Mainz, Germany
[4]Leibniz Institute for Resilience Research Mainz, Germany

Address:
Radboud University Nijmegen
Donders Centre for Cognition
Thomas van Aquinostraat 4
6525GD, Nijmegen, The Netherlands
Email: benjamin.kop@donders.ru.nl

Abstract

Transcranial ultrasonic stimulation (TUS) is rapidly emerging as a promising non-invasive neuromodulation technique. TUS is already well-established in animal models, and now stimulation protocols that optimize neuromodulatory efficacy for human application are required. One promising protocol, pulsed at 1000 Hz, has consistently resulted in motor cortical inhibition. At the same time, a parallel research line has highlighted the potentially confounding influence of peripheral auditory stimulation arising from pulsing TUS at audible frequencies. Across four experiments, one preregistered, at three independent institutions, we employed tightly matched control conditions to disentangle direct neuromodulatory effects of TUS from those driven by the salient auditory confound in a combined transcranial ultrasonic and magnetic stimulation paradigm. We replicated motor cortical inhibition following TUS, but showed through both controls and manipulation of stimulation intensity, duration, and auditory masking conditions that this inhibition was driven by peripheral auditory stimulation rather than direct neuromodulation. This study highlights the substantial impact of the auditory confound, invites a reevaluation of prior findings, and calls for appropriate control conditions in future TUS work. Only when direct effects are disentangled from those driven by peripheral confounds can TUS fully realize its potential for neuroscientific research and clinical applications.

Keywords: transcranial ultrasonic stimulation, motor cortical excitability, auditory confound

Introduction

Modulating neural activity is a powerful tool for causal inference that advances our understanding of the brain and holds great clinical potential (Bergmann & Hartwigsen, 2021; Bestmann & Walsh, 2017). Transcranial ultrasonic stimulation (TUS) is positioned to be a transformative non-invasive neuromodulation technique with unprecedented spatial resolution and depth range (Darmani et al., 2022). The efficacy of this technique is well-established in cell cultures and animal models (Menz et al., 2013; Mohammadjavadi et al., 2019; Murphy et al., 2022; Tyler et al., 2008, 2018; Yoo et al., 2022), and emerging evidence for the neuromodulatory utility of TUS in humans has been reported for both cortical and subcortical structures (cortical: Braun et al., 2020; Fomenko et al., 2020; Lee et al., 2016; Legon, Bansal, et al., 2018; Liu et al., 2021; Zeng et al., 2022; subcortical: Ai et al., 2016; Cain et al., 2021; Legon, Ai, et al., 2018; Monti et al., 2016). In the current foundational stage of TUS for human applications, it is essential to converge on protocols that maximize the specificity and efficacy of stimulation (Folloni et al., 2019; Verhagen et al., 2019).

Here, we show that previously reported motor inhibitory effects following a conventional 1000 Hz pulsed repetition frequency (PRF) protocol largely arise from indirect auditory stimulation rather than direct neuromodulation, bringing the efficacy of this commonly applied protocol into question. Motor inhibitory effects of 1000 Hz TUS are one of the most robust and replicable findings in the human literature (Fomenko et al., 2020; Legon, Bansal, et al., 2018; Xia et al., 2021). However, recent studies in both animal and human models demonstrate how electrophysiological and behavioral outcomes can be elicited by nonspecific auditory activation rather than direct neuromodulation (Airan & Butts Pauly, 2018; Braun et al., 2020; Guo et al., 2018; Sato et al., 2018). Notably, the presence and salience of these auditory confounds strongly depend on the applied pulsing frequency and physical characteristics of the ultrasound transducer. Indirect effects of stimulation are not unique to TUS, as transcranial magnetic and electric stimulation are also associated with auditory and somatosensory confounds. Indeed, the field of non-invasive brain stimulation depends on controlling for these confounding factors, when present, to unveil the specificity of the neuromodulatory effects (Conde et al., 2019; Duecker et al., 2013; Polanía et al., 2018; Siebner et al., 2022). In this study, we quantified the effect of TUS on motor cortical excitability while tightly controlling for confounding factors; an approach that is essential for this new technique to reach its full potential.

Fundamental investigations into the neurophysiological effects of TUS on motor cortical excitability in humans have been conducted using a combined TUS and transcranial magnetic stimulation (TMS) approach, pioneered by Legon and colleagues (2018). Using motor-evoked potentials (MEPs) as a readout of corticospinal excitability, these studies reported an inhibitory effect of online 1000 Hz pulsed TUS on MEPs (Fomenko et al., 2020; Legon, Bansal, et al., 2018; Xia et al., 2021). They further highlight the impact of ultrasonic stimulation parameters on the modulation of cortical excitability, emphasizing the importance of pulsing frequency, duty cycle, and stimulus duration (Fomenko et al., 2020). However, the mechanism by which TUS evokes motor inhibition remains under debate (Xia et al., 2021). Here, we demonstrate that some of these previously reported effects might be driven by preparatory motor inhibition cued by nonspecific auditory confounds inherent to this pulsed ultrasonic stimulation protocol.

In four experiments conducted across three institutions, we interrogated the role of the auditory confound in the context of TUS-induced inhibition of TMS-evoked MEPs (***Figure 1***). We first replicated the core finding of motor cortical inhibition following TUS, where we additionally included

strict controls to better isolate the impact of the auditory confound. These controls involved stimulation of tightly matched control sites and administration of an auditory stimulus alone. We examined the effects of TUS at multiple stimulation intensities, stimulus durations, and both with and without auditory masking stimuli. We further tested whether auditory characteristics such as duration, pitch, and volume might differentially affect motor excitability. Across these four experiments, we are positioned to observe a spatially specific effect of TUS over and above auditory and potentially somatosensory confounds, and further characterize how these confounds might impact motor cortical excitability.

In line with prior work, we found an inhibition of motor cortical excitability following only longer durations of TUS. However, this effect was also observed following stimulation of a control site and administration of a sound in the absence of TUS. We observed no evidence for an underlying specific neuromodulatory effect of TUS when examining a dose-response effect of TUS, nor when an effective masking stimulus was administered. Instead, our results provide evidence that auditory cueing, rather than direct neuromodulation, underlies the observed motor cortical inhibition. Indeed, the characteristics of auditory stimuli including duration, pitch, and audibility in general affected cortical excitability differentially. The present study highlights the importance of carefully constructed control conditions to account for confounding factors while exploring and refining TUS as a promising technique for human neuromodulation.

Results

Overview of experiments

	stimulation condition	free-water intensity (I_{sppa})	auditory masking	TUS duration
Exp. I	on-target TUS active control TUS sound-sham baseline	32.5 W/cm² 65 W/cm²	time-locked to TUS no mask masked	100 ms 500 ms
Exp. II *preregistered*	on-target TUS active control TUS sound-sham baseline	6.35 W/cm² 19.06 W/cm²	time-locked to TUS no mask masked	500 ms
Exp. III	on-target TUS sound-sham baseline	9.26 W/cm²	time-locked to TUS masked 1 kHz, 500 ms 1 kHz, 700 ms 12 kHz, 500 ms 12 kHz, 700 ms	500 ms
Exp. IV	inactive control TUS baseline	4.34 W/cm² 8.69 W/cm² 10.52 W/cm²	continuous masking no mask masked	400 ms

Figure 1. Overview of experimental conditions. For each experiment (row), core experimental conditions are noted. In Experiments I and II, main conditions included on-target TUS (left-hemispheric hand motor area), active control TUS (right-hemispheric face motor area), sound-sham (auditory stimulation alone), and baseline (TMS only). Here, TUS was applied at two stimulation intensities, and both with and without a time-locked auditory masking stimulus. We report the spatial-peak pulse-averaged intensity in free-water without attenuation from biological tissue. Please see ***Figure 5*** for estimations of intracranial intensities. In Experiment I, TUS was further administered at both 100 and 500 ms stimulus durations. Experiment II is a preregistered study to confirm and extend the findings of Experiment I. In Experiment III, four auditory stimuli of varying pitch and duration were administered both in isolation (sound-sham) and alongside on-target TUS. In Experiment IV, inactive control TUS was administered to the white matter ventromedial to the hand motor area at three intensities (i.e., auditory confound volumes) both with and without a continuous auditory masking stimulus.

Replication of motor cortical inhibition following TUS (Experiments I-III)

We corroborate previous reports of MEP suppression following 500 ms of TUS applied over the hand motor area (***Figure 2***; Fomenko et al., 2020; Legon, Bansal, et al., 2018; Xia et al., 2021). A linear mixed model comparing 500 ms of on-target TUS to baseline revealed significantly lower MEP amplitudes following TUS for Experiment I (b = -0.14, SE = 0.06, $t(11)$ = -2.23, p = 0.047), Experiment II (b = -0.18, SE = 0.04, $t(26)$ = -4.82, $p = 6 \cdot 10^{-5}$), and Experiment III (b = -0.22, SE = 0.07, $t(15)$ = -3.08, p = 0.008).

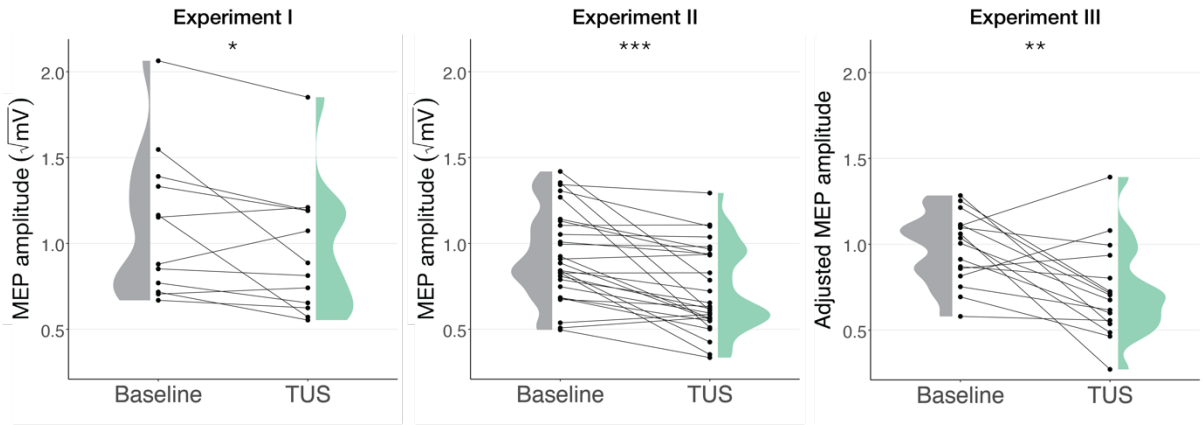

Figure 2. 500 ms of on-target TUS significantly attenuates MEP amplitude. Points represent individual participants, clouds depict the distribution across participants, and asterisks reflect significance level: *p < 0.05, **p < 0.01, ***p < 0.001.

Motor cortical inhibition is not specific to on-target TUS (Experiments I-IV)

In addition to ultrasonic stimulation of the hand motor area, we also included control and sound-sham conditions. Much like our observations for on-target TUS, linear mixed models comparing each of these conditions to baseline revealed a significant reduction in MEP amplitude (***Figure 3***). In Experiments I, II, and III, presentation of a sound alone (i.e., sound-sham) attenuated MEP amplitude (Experiment I: b = -0.14; SE = 0.05; $t(11)$ = -3.18; p = .009; Experiment II: b = -0.22; SE = 0.04; $t(26)$ = -5.38; $p = 1 \cdot 10^{-5}$; Experiment III: b = -0.24; SE = 0.08; $t(15)$ = -2.86; p = 0.012). Stimulation of the contralateral face area also resulted in motor cortical inhibition in Experiments I and II (Experiment I: b = -0.12, SE = 0.05, $t(11)$ = -2.29, p = 0.043; Experiment II: b = -0.22, SE = 0.04, $t(26)$ = -5.60, $p = 7 \cdot 10^{-6}$), as did stimulation of the white matter ventromedial to the hand motor area in Experiment IV (b = -0.14; SE = 0.04; $t(11)$ = -3.09; p = 0.010). These results suggest a spatially non-specific effect of TUS that is related to the auditory confound.

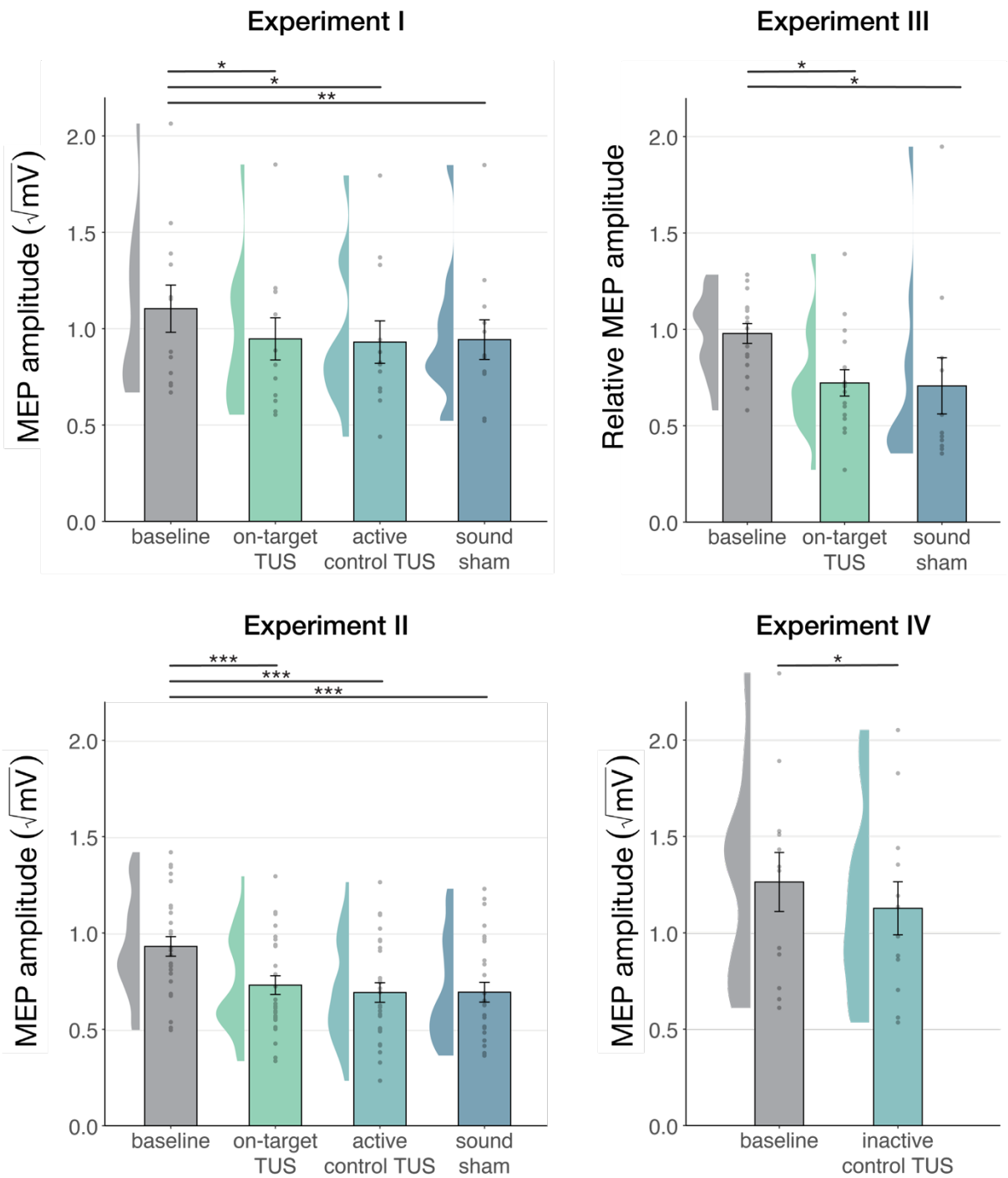

Figure 3. Nonspecific attenuation of MEP amplitude. A significant suppression of MEP amplitude relative to baseline (gray) was observed for on-target TUS (green), but also for stimulation of a control region (cyan), and presentation of a sound alone (sound-sham; blue) indicating a spatially non-specific and sound-driven effect on motor cortical excitability. Bar plots depict condition means, error bars represent standard errors, clouds indicate the distribution over participants, and points indicate individual participants. Square-root corrected MEP amplitudes are depicted for Experiments I, II, and IV, and *Relative MEP amplitude* is depicted for Experiment III (see ***Methods***). *p < 0.05, **p < 0.01, ***p < 0.001

No dose-response effect of stimulation intensity (Experiments I-II)

We further tested for direct ultrasonic neuromodulation by investigating a potential dose-response effect of TUS intensity (I_{sppa}) on motor cortical excitability. First, we applied TUS at multiple free-water stimulation intensities (**Figure 4A**). In Experiment I, a linear mixed model with the factor 'intensity' (32.5/65 W/cm^2) did not reveal a significant effect of different on-target TUS intensities on motor excitability ($F(1,11) = 0.47$, $p = 0.509$, $\eta_p^2 = 0.04$). In Experiment II, a linear mixed model with the factors 'stimulation site' (on-target/active control), 'masking' (no mask/masked), and intensity (6.35/19.06 W/cm^2) similarly did not reveal a significant effect of stimulation intensity on motor excitability ($F(1,50) = 1.29$, $p = 0.261$, $\eta_p^2 = 0.03$). Importantly, there was no effect of stimulation site ($F(1,168) = 1.75$, $p = 0.188$, $\eta_p^2 = 0.01$), nor any significant interactions (all p-values > 0.1; all $\eta_p^2 < 0.06$). These results provide neither evidence for spatially specific neuromodulation when directly comparing stimulation sites, nor evidence for a dose-response relationship within the range of applied intensities.

However, it is likely that the effectiveness of TUS depends primarily on the realized intracranial intensity at the target, which can vary greatly between individuals as a function of multiple properties such as skull morphology and acoustic properties. We therefore estimated realized intracranial intensity, along with other indices, with individualized 3D simulations (***Figure 5***). Thermal and mechanical indices fell within internationally recognized safety guidelines for diagnostic ultrasound, including those conventionally used in TUS research (***Figure 5C***; United States Food and Drug Administration, 2017; Pasquinelli et al., 2019). See ***Supplementary Table 1*** and ***Supplementary Figures 1-4*** for all simulation outputs.

As Experiment II had a sufficient sample size to assess inter-individual variability, we assessed the dose-response function of MEP amplitude following on-target TUS expressed as a percentage of baseline, active control, and sound-sham conditions against simulated intracranial intensities (**Figure 4B**). Simple linear models predicting percentage change from these three conditions revealed a significant positive relationship for MEP amplitude change following on-target TUS from baseline for 6.35 W/cm^2 free-water stimulation ($b = 19.46$, $SE = 7.91$, $t(24) = 2.46$, $p = 0.022$), and a positive trend for 19.06 W/cm^2 free-water stimulation ($b = 5.77$, $SE = 3.01$, $t(24) = 1.92$, $p = 0.067$). However, no significant relationship was observed for MEP amplitude change from active control (free-water 6.35 W/cm^2: $b = -1.02$, $SE = 3.66$, $t(24) = -0.28$, $p = 0.783$; free-water 19.06 W/cm^2: $b = 0.04$, $SE = 1.66$, $t(24) = 0.02$, $p = 0.983$) or sound-sham conditions (free-water 6.35 W/cm^2: $b = 0.58$, $SE = 4.78$, $t(24) = 0.12$, $p = 0.904$; free-water 19.06 W/cm^2: $b = -0.66$, $SE = 1.92$, $t(24) = -0.35$, $p = 0.733$). Indeed, these results do not provide evidence for a dose-response relationship of on-target TUS. Instead, they suggest that the auditory confound volume and salience may be relevant.

Where less acoustic energy was delivered to the brain, more acoustic energy was absorbed by the skull. This energy is thought to propagate via shear waves to the cochlea (Braun et al., 2020; Salahshoor et al., 2020), particularly when square wave amplitude modulation is administered as in the present study. With greater energy deposition in the skull, increased amplitude shear waves would likely result in greater perceived sound volumes (Stenfelt & Håkansson, 2002). These higher auditory confound volumes could elicit stronger MEP attenuation. Indeed, lower intracranial intensities (i.e., higher energy deposition in the skull) show stronger MEP attenuation, pointing towards a role of perceived confound volume. Importantly, if the observed motor inhibition was driven by ultrasonic neuromodulation rather than an auditory confound, we would have expected stronger MEP attenuation at higher intracranial intensities when compared to baseline, but also compared to active control and sound-sham conditions.

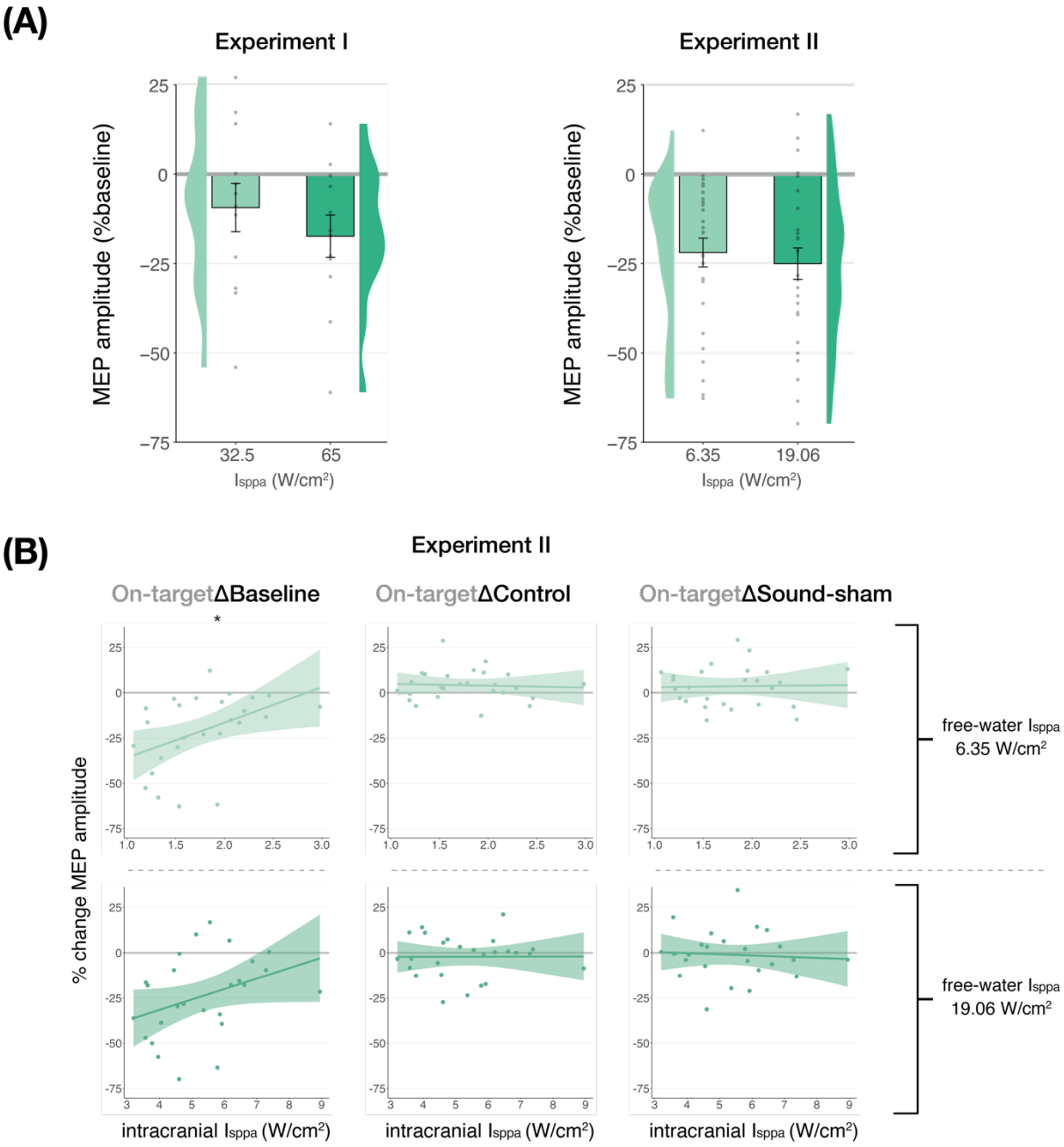

Figure 4. No dose-response effects of TUS. (A) There is no significant effect of free-water stimulation intensity on MEP amplitude in Experiments I or II. Values are expressed as a percentage of baseline MEP amplitude (square root corrected). All conventions are as in Figure 3. **(B)** We estimate the dose-response relationship for simulated intracranial intensity. Percentage change of MEP amplitude for on-target TUS from baseline (left), active control (middle), and sound-sham (right), for the two applied free-water intensities: 6.35 W/cm^2 (top) and 19.06 W/cm^2 (bottom). The shaded area represents the 95% CI, points represent individual participants.

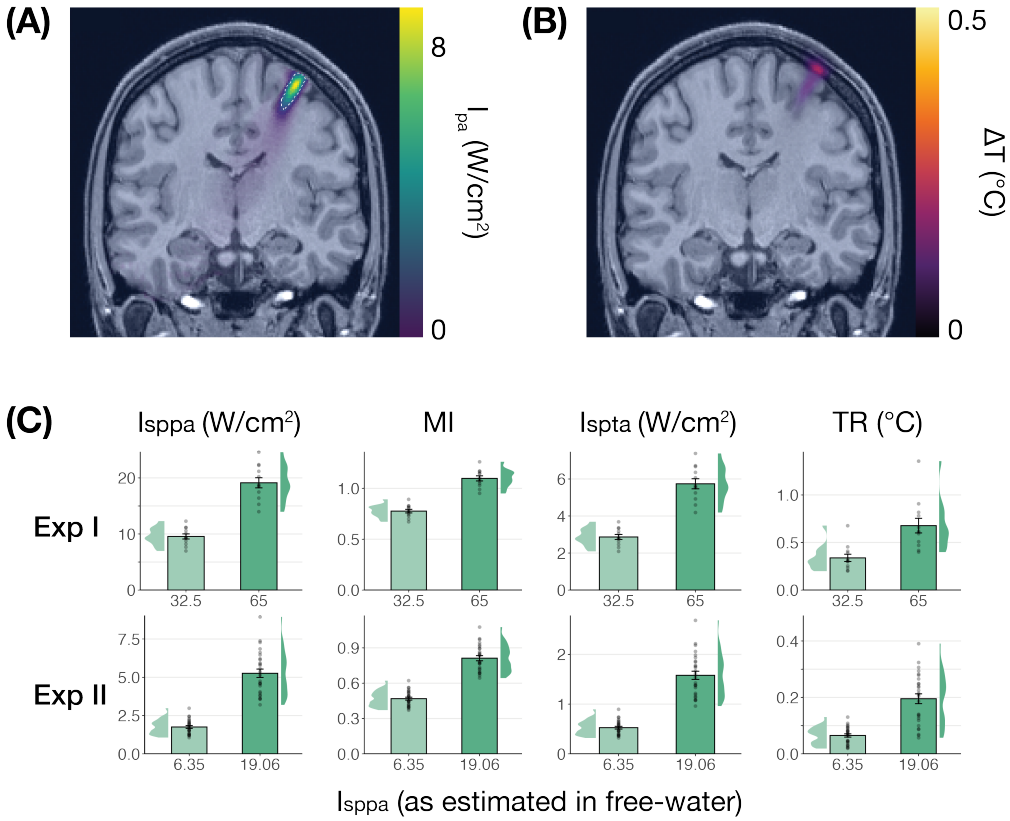

Figure 5. Acoustic and thermal simulations of TUS. **(A)** Acoustic simulation depicting the estimated pulse-average intensity (I_{pa}) for a single subject in Experiment II. Intensities are depicted above a 0.15 W/cm^2 lower bound, with the dotted line indicating the full-width half-maximum of the pressure. **(B)** Thermal simulation depicting the estimated maximum temperature rise for a single subject in Experiment II. **(C)** Simulated indices for Experiment I (top) and Experiment II (bottom) for both applied free-water stimulation intensities including spatial-peak pulse- and temporal-average intensity (I_{sppa}, I_{spta}), the mechanical index (MI), and peak thermal rise (TR). Conventions are as in Figure 3.

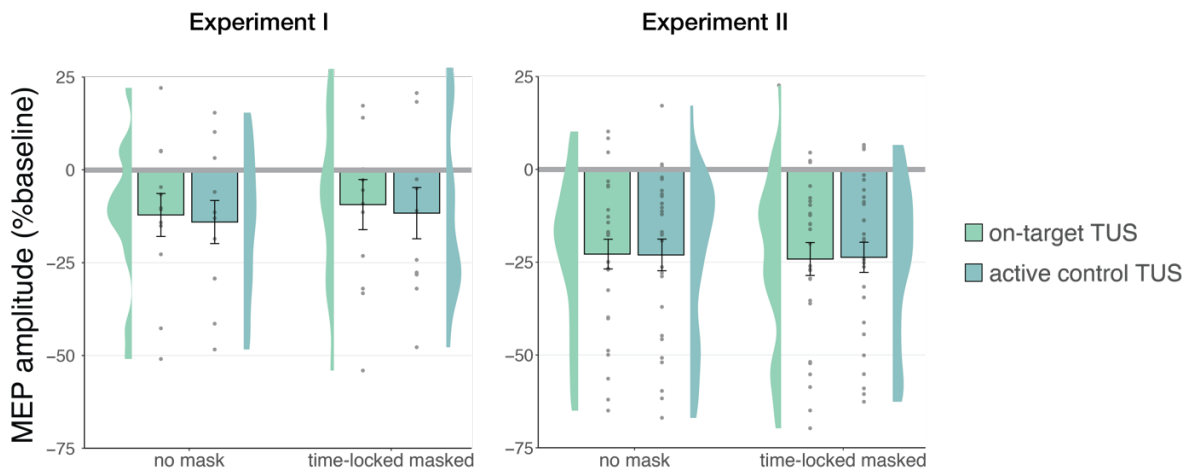

Figure 6. Time-locked auditory masking. There is no significant main effect or interaction between stimulation site (on-target/active control) and masking, indicating that audible differences between stimulation sites did not obscure or explain the absence of evidence for direct neuromodulation. All conventions are as in Figure 3.

Audible differences between stimulation sites do not underlie nonspecific inhibition (Experiments I-II)

We have shown that the auditory confound associated with 1000 Hz pulsed TUS, or even sound alone, can affect motor cortical excitability. It follows that different auditory stimuli might differentially affect cortical excitability, where stimulation over two separate sites could evoke distinct perceptual experiences, for example based on differences in bone-conducted sound (Braun et al., 2020). To account for possible audibility differences between stimulation of on-target and active control sites in Experiments I and II, we also tested these conditions in the presence of a time-locked masking stimulus (***Figure 6***). In Experiment I, a linear mixed model with factors 'masking' (no mask/masked) and 'stimulation site' (on-target/active control) did not reveal a significant effect of masking ($F(1,11) = 0.01$, $p = 0.920$, $\eta_p^2 = 1{\cdot}10^{-5}$), stimulation site ($F(1,11) = 0.15$, $p = 0.703$, $\eta_p^2 = 0.01$), nor their interaction ($F(1,11) = 1{\cdot}10^{-3}$, $p = 0.971$, $\eta_p^2 = 1{\cdot}10^{-4}$). Similarly, in Experiment II, the linear mixed model described under the previous section revealed no significant main effect of masking ($F(1,30) = 1.68$, $p = 0.205$, $\eta_p^2 = 0.05$), nor any interactions (all p-values > 0.1; all $\eta_p^2 < 0.06$). These results indicate that an underlying specific neuromodulatory effect of TUS was not being obscured by audible differences between stimulation sites.

Blinding efficacy of auditory masking (Experiment II)

In Experiment II, we further investigated whether participants were effectively blinded to ultrasonic stimulation when this time-locked auditory masking stimulus was applied (***Figure 7A***). A logistic mixed effects model predicting response (stimulation yes/no) by factors 'stimulation site' (on-target/active control), 'intensity' (6.35/19.06 W/cm^2), and 'masking' (no mask/masked) with random intercepts by participant revealed significantly lower detection rates when masking was applied ($b = -0.90$, $SE = 0.31$, $z = -2.87$, $p = 0.004$), but showed no significant effect of stimulation site ($b = 0.05$, $SE = 0.31$, $z = 0.16$, $p = 0.875$) or intensity ($b = 0.30$, $SE = 0.31$, $z = 0.95$, $p = 0.342$), nor any significant interactions (all $p > 0.6$). Only ultrasonic stimulation applied at higher intensities (19.06 W/cm^2) in the absence of an auditory masking stimulus were detected by participants at an above-chance rate (i.e., 50%; on-target: $Z = 2.6$, $p = 0.011$; active control: $Z = 2.9$, $p = 0.004$). Detection rates for lower intensities, masked stimulation, and sound-sham conditions did not differ significantly from chance, as revealed by post-hoc one-sample Wilcoxon signed rank tests (all $Z < 1.7$, $p > 0.09$). Taken together, these results show that the masking used in Experiment II successfully reduced participants' ability to determine whether they had received stimulation.

It is possible that, while blinding to TUS versus no-TUS is successful for explicit judgements, slight audibility differences between on-target and active control stimulation persist even when stimulation is masked. A two-way repeated measures ANOVA revealed that masked stimulation over the two different sites sounded less similar than masked stimulation over the same site (***Figure 7B***; $F(1,26) = 14.00$, $p = 9{\cdot}10^{-4}$) while no significant main effect of, or interaction with, intensity was observed (main effect: $F(1,26) = 1.98$, $p = 0.171$; interaction: $F(1,26) = 0.26$, $p = 0.613$). These results suggest that, while masking may effectively blind participants, reducing detection of ultrasonic stimulation, slight audible differences between different stimulation sites may persist.

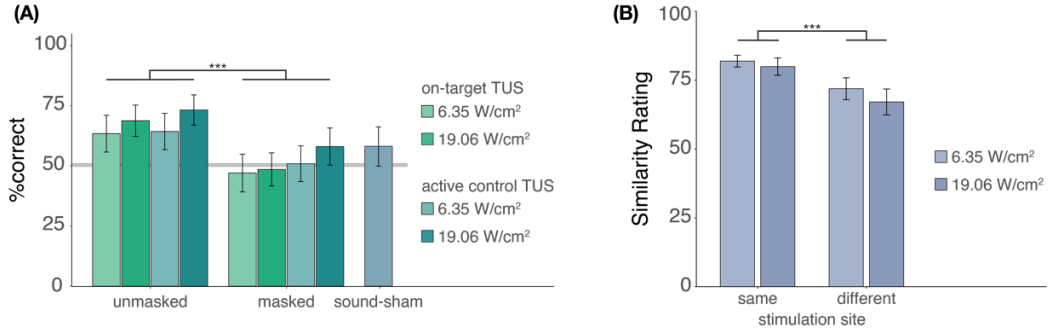

Figure 7. Blinding efficacy. (A) An auditory masking stimulus significantly decreased participants' ability to determine whether they had received ultrasonic stimulation. **(B)** However, when masked stimulation was applied over different sites, participants still rated these stimuli as sounding less similar than stimulation applied over the same site. Bars represent means across participants, error bars represent the standard error, and points represent individual participants.

Stimulus duration dependency of MEP attenuation is not unique to TUS (Experiment I)

Prior research has shown that longer durations of TUS significantly inhibited motor cortical excitability (i.e., ≥400 ms; Fomenko et al., 2020), while shorter durations did not. In Experiment I, we applied on-target, active control, and sound-sham conditions at shorter and longer durations to probe this effect. When directly comparing these conditions at different stimulus durations (100/500 ms), no evidence for an underlying neuromodulatory effect of TUS was observed, in line with our previous findings. Instead, a linear mixed model with factors 'condition' (on-target/active control/sound-sham) and 'stimulus duration' (100/500 ms) revealed only a significant main effect of (auditory) stimulus duration, where longer stimulus durations resulted in stronger MEP attenuation ($F(1,11) = 10.07$, $p = 0.009$, $\eta_p^2 = 0.48$). There was no significant effect of condition ($F(2,11) = 1.30$, $p = 0.311$, $\eta_p^2 = 0.19$), nor an interaction between stimulus duration and condition ($F(2,11) = 0.65$, $p = 0.543$, $\eta_p^2 = 0.11$). These results further show that the auditory confound and its timing characteristics, rather than ultrasonic neuromodulation, underlies the observed inhibition of motor cortical excitability (***Figure 8***).

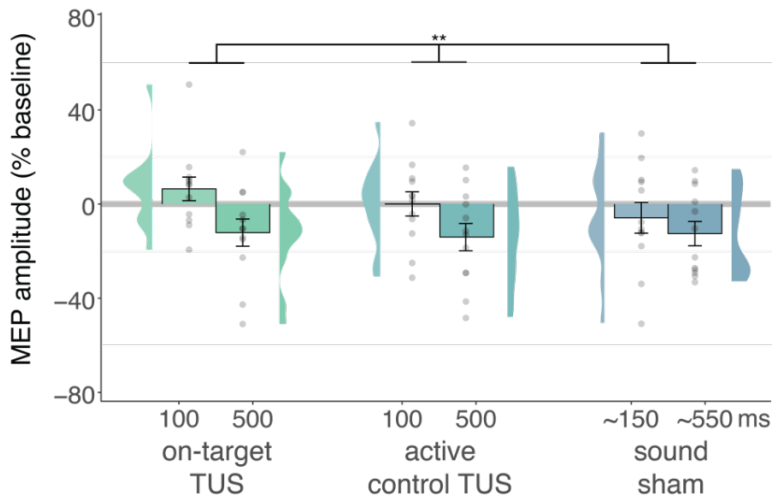

Figure 8. Effect of stimulus duration on MEP amplitude across conditions. Longer stimulus durations resulted in lower MEP amplitudes. There was no effect of condition (on-target/active control/sound-sham) nor an interaction between condition and stimulus duration. All conventions are as in Figure 3.

Auditory characteristics can affect motor excitability (Experiment III)

In Experiment III, we further investigated the effects of auditory characteristics on motor excitability by varying the duration and pitch of sound-sham (500 and 700 ms; 1 and 12 kHz). In the first test, 500 ms of auditory stimulation resulted in lower MEPs than 700 ms (***Figure 9A***; $F(1,15) = 7.12$, $p = 0.017$, $\eta_p^2 = 0.32$). There was no significant effect of pitch ($F(1,15) = 0.02$, $p = 0.878$, $\eta_p^2 = 2{\cdot}10^{-3}$), nor an interaction between pitch and duration ($F(1,15) = 2.23$, $p = 0.156$, $\eta_p^2 = 0.13$).

Subsequently, ultrasonic stimulation was also administered alongside these four auditory stimuli. Here, a linear mixed model with factors 'auditory stimulus duration' (500/700 ms), 'pitch' (1/12 kHz), and 'ultrasonic stimulation' (yes/no) revealed no significant effect of auditory stimulus duration in contrast to the first test (***Figure 9B***; $F(1,15) = 0.44$, $p = 0.517$, $\eta_p^2 = 0.03$). However, a 1 kHz pitch resulted in significantly lower MEP amplitudes than a 12 kHz pitch ($F(1,15) = 4.94$, $p = 0.042$, $\eta_p^2 = 0.25$). Importantly, we find no evidence for ultrasonic neuromodulation, where both on-target TUS and sound-sham reduced MEP amplitude from baseline (***Figure 2-3***), and where applying on-target TUS did not significantly affect MEP amplitude as compared to sound-sham ($F(1,15) = 0.42$, $p = 0.526$, $\eta_p^2 = 0.03$; ***Figure 9B***). We observed a nonsignificant trend for the interaction between 'ultrasonic stimulation' and 'auditory stimulus duration' ($F(1,15) = 4.22$, $p = 0.058$, $\eta_p^2 = 0.22$). No trends were observed for the remaining interactions between these three factors (all $\eta_p^2 < 0.06$, $p > 0.3$). Taken together, these results do not provide evidence for direct ultrasonic neuromodulation but support the influence of auditory stimulation characteristics on motor cortical excitability.

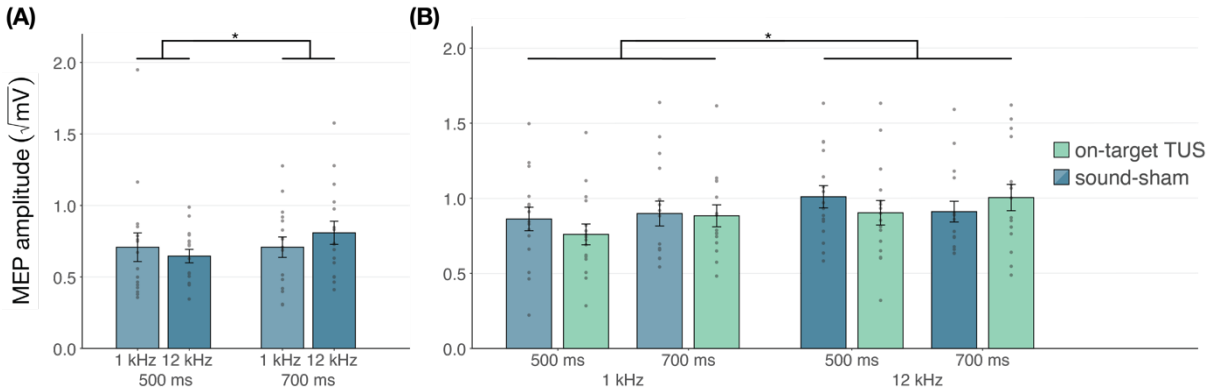

Figure 9. Effects of auditory characteristics on MEP amplitudes. (A) In the first experimental test, significantly lower MEP amplitudes were observed following a 500 ms auditory stimulus as compared to a 700 ms auditory stimulus. **(B)** In the second test, significantly lower MEP amplitudes were observed following a 1 kHz pitch as compared to a 12 kHz pitch. There was no effect of ultrasonic stimulation. All conventions are as in Figure 3.

Audibility of TUS contributes to motor inhibition (Experiment IV)

To further probe the audibility of TUS in relation to motor cortical inhibition, we applied TUS to an inactive target – the white matter ventromedial to the left-hemispheric hand motor area – both with and without a continuous auditory masking stimulus. MEP amplitudes did not significantly differ in baseline conditions (i.e., TMS only) regardless of whether a continuous sound was being played ($b = 0.03$, $SE = 0.06$, $t(11) = 0.52$, $p = 0.616$), indicating that continuous auditory stimulation alone might not be sufficient to inhibit MEP amplitude.

In addition to applying TUS with and without continuous masking, we applied stimulation at multiple intensities, allowing us to isolate the effect of the auditory confound and its volume while minimizing the possibility of direct ultrasonic neuromodulation. A linear mixed model with factors 'masking' (no mask/masked) and 'intensity' (4.34/8.69/10.52 Wcm^{-2}) with a random intercept and slope for each factor revealed a significant interaction ($F(2,4038) = 3.43$, $p = 0.033$, $\eta_p^2 = 2 \cdot 10^{-3}$) and an accompanying effect of 'masking' with lesser MEP attenuation when stimulation was masked ($F(1,11) = 11.84$, $p = 0.005$, $\eta_p^2 = 0.52$; ***Figure 10***). Follow-up comparisons revealed significantly less attenuation for masked stimulation at 4.34 W/cm^2 intensity ($F(1,11) = 13.02$, $p = 0.004$, $\eta_p^2 = 0.55$), and a nonsignificant trend for the higher intensities (8.69 W/cm^2: $F(1,11) = 3.87$, $p = 0.077$, $\eta_p^2 = 0.27$; 10.52 W/cm^2: $F(1,11) = 3.47$, $p = 0.089$, $\eta_p^2 = 0.24$). In direct comparisons to baseline, all conditions resulted in a significant inhibition of MEP amplitude (all $t < -3.36$, all $p < 0.007$), with the exception of continuously masked stimulation at the lowest intensity of 4.34 W/cm^2 I_{sppa} ($b = -0.06$, $SE = 0.03$, $t(11) = -2.04$, $p = 0.065$).

Taken together, the data indicate that continuous masking results in reduced motor inhibition, likely owing to the minimized audibility of TUS, particularly when applied at a lower stimulation intensity (i.e., auditory confound volume). It is possible that the remaining motor inhibition observed during masked trials owes to, albeit decreased, persistent audibility of TUS over and above the continuous auditory mask. Indeed, MEP attenuation in the masked conditions descriptively scale with participant reports of audibility, where lower stimulation intensities are more often experienced as inaudible and exhibit less inhibition, while higher intensities are less often experienced as inaudible and exhibit more inhibition (***Supplementary Figure 5***).

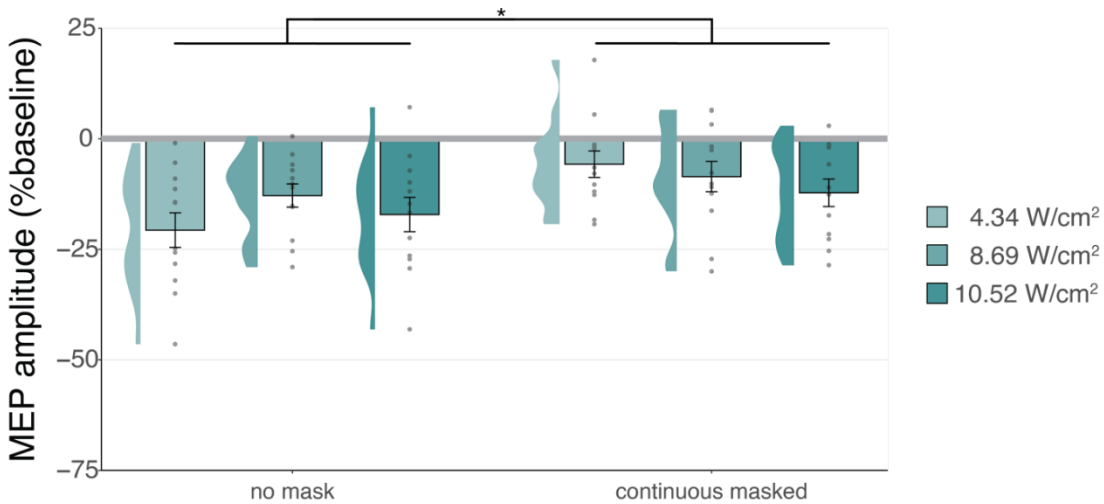

Figure 10. Motor inhibition as a function of TUS audibility. Significantly less MEP attenuation was observed when stimulation was continuously masked, particularly for low stimulation intensities, pointing towards a role of TUS audibility in MEP reduction. All conventions are as in Figure 3.

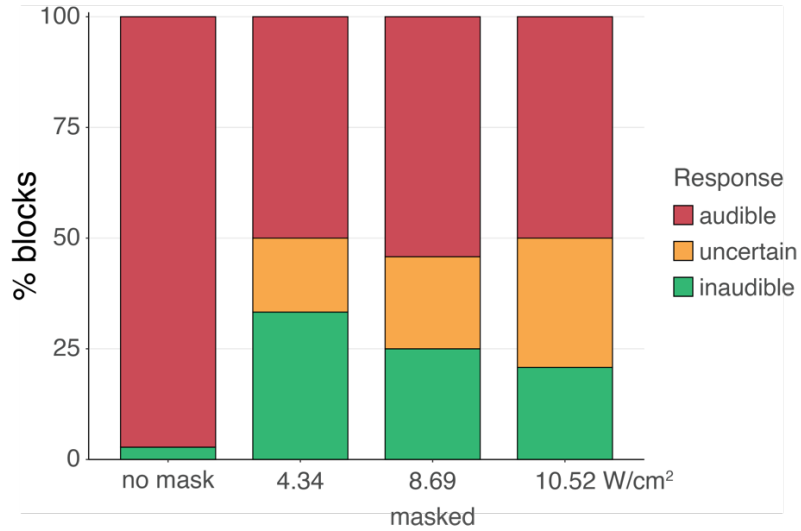

Supplementary Figure 5. Subjective report of TUS audibility. Descriptively, when no mask was applied, TUS was audible (red) in nearly all cases. During continuous masking, TUS was experienced as inaudible (green) less often at higher stimulation intensities.

Preparatory learning may explain motor inhibition (Experiments I-II)

In this study, we find nonspecific motor inhibitory effects of TUS that are dependent upon characteristics of auditory stimuli, providing strong evidence that MEP attenuation results from sound cueing rather than direct neuromodulation. Two putative mechanisms through which sound cuing may drive motor inhibition have been proposed, focusing either on the learned compensatory processes (Capozio et al., 2021; Tran et al., 2021a), or on a startle response leading to global inhibition (Fisher et al., 2004; Furubayashi et al., 2000; Ilic et al., 2011; Kohn et al., 2004; Wessel & Aron, 2013). Critically, we can dissociate between these theories by exploring the temporal dynamics of MEP attenuation. First, auditory cueing may allow participants to learn when the TMS pulse will be administered, resulting in compensatory processes to drive in MEP reduction in preparation for the upcoming TMS pulse (Capozio et al., 2021; Tran et al., 2021b). In this scenario, MEP amplitudes should decrease over time, as the relative timing of TUS and TMS is being learned, followed by a stabilization at a decreased MEP amplitude once this relationship has been learned. Second, auditory stimulation may lead to a startle response resulting in global inhibition (Fisher et al., 2004; Furubayashi et al., 2000; Ilic et al., 2011; Kohn et al., 2004; Wessel & Aron, 2013). In this case, one would expect the startle response to habituate over time, where MEP attenuation would initially be reduced, followed by a normalization throughout the course of the experiment.

In Experiments I and II, linear mixed models with 'trial number' as a predictor show significant changes in MEP amplitude throughout the experiment, pointing to a learning effect. Specifically, in Experiment I, a significant reduction in MEP amplitude was observed across the first 10 trials where a 500 ms stimulus is delivered (b = -0.04, SE = 0.01, $t(11)$ = -2.88, p = 0.015), following by a stabilization in subsequent blocks ($b = -2\cdot10^{-4}$, $SE = 3\cdot10^{-4}$, $t(11)$ = -0.54, p = 0.601). This same pattern was observed in Experiment II, with a significant reduction across the first 20 trials (b = -0.01, $SE = 3\cdot10^{-3}$, $t(26)$ = -4.08, $p = 4\cdot10^{-4}$), followed by stabilization ($b = 6\cdot10^{-5}$, $SE = 1\cdot10^{-4}$, $t(26)$ = 0.46, p = 0.650; ***Figure 11***). These results could reflect a learning process whereby TUS predicts TMS, leading to a compensatory expectation-based reduction of motor excitability.

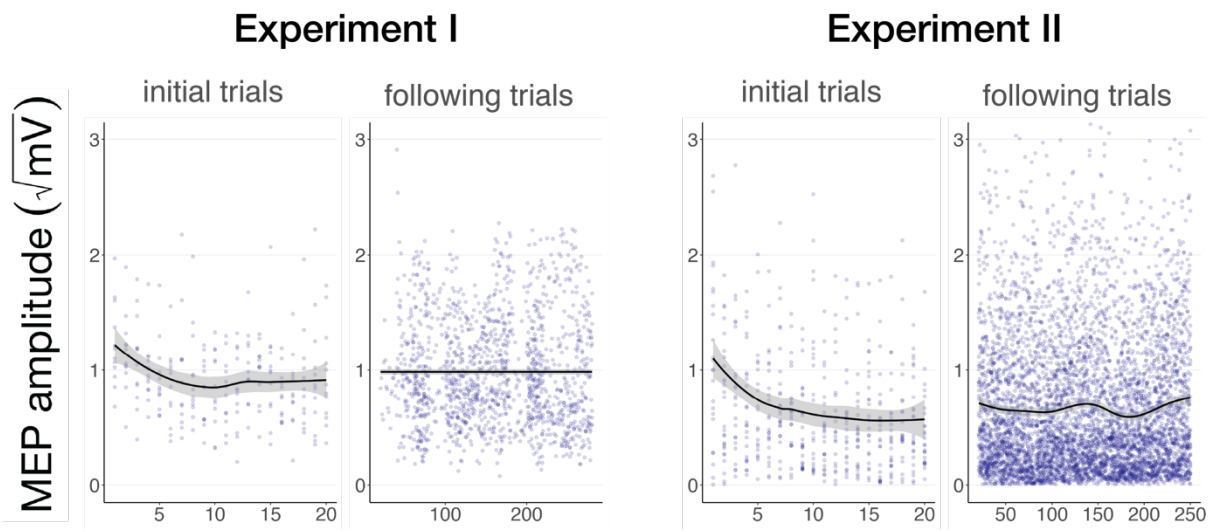

Figure 11. Auditory cueing of TMS. There was a significant reduction in MEP amplitude when participants were first presented with a 500 ms stimulus (initial trials) in Experiment I (left) and Experiment II (right), following by a stabilization of MEP amplitude during the rest of the experiment (following trials), indicating a learning process by which TUS acts as a cue signaling the onset of TMS. The solid line depicts the loess regression fit, and the shaded area represents the 95% confidence interval.

Discussion

In this study, we show the considerable impact of auditory confounds during audibly pulsed TUS in humans. We employed carefully constructed control conditions to account for auditory contributions during ultrasonic neuromodulation of motor cortical excitability across four experiments, one preregistered, at three independent institutions. While we corroborated the robust and consistent finding of motor inhibition during TUS (Fomenko et al., 2020; Legon, Bansal, et al., 2018; Xia et al., 2021), we demonstrated that this inhibition also occurs with stimulation of a control region or presentation of a sound alone, suggesting that the auditory confound rather than direct ultrasonic neuromodulation drives inhibition. Further, no direct neuromodulatory effects were observed, regardless of stimulation timing, intensity, or masking. Instead, we found evidence that characteristics of auditory stimuli do affect motor excitability. Our results call for a reevaluation of earlier findings following audible TUS, and highlight the importance of suitable controls in experimental design (Bergmann & Hartwigsen, 2021; Siebner et al., 2022).

No evidence for direct neuromodulation by TUS

Across four experiments, we build on prior accounts of sound-driven effects of TUS in behavioral and electrophysiological research (Airan & Butts Pauly, 2018; Braun et al., 2020; Guo et al., 2018; Johnstone et al., 2021; Sato et al., 2018). Here, we assessed ultrasonic and auditory contributions to the effects of a conventional 1000 Hz pulsed TUS protocol on TMS-evoked MEPs, which has consistently resulted in motor cortical inhibition of the hand motor area (Fomenko et al., 2020; Legon, Bansal, et al., 2018; Xia et al., 2021). While we successfully replicated this inhibitory effect (***Figure 2***), we found the same inhibition following stimulation of a motor control site (contralateral, active) and stimulation of a white-matter control site (ipsilateral, inactive; ***Figure 3***). This contrasts to a prior study where stimulation of the contralateral hand motor area did not disrupt motor cortical excitability (Xia et al., 2021). Indeed, in all direct comparisons between on-target and control stimulation, no differences in excitability were observed, pointing towards a spatially nonspecific effect of TUS. We further observed an inhibitory effect following administration of an auditory stimulus alone, suggesting that online TUS motor inhibition is largely driven by the salient auditory confound, rather than spatially specific and direct neuromodulation.

Consistent with this interpretation, we found no evidence of a dose-response relationship between TUS intensity (I_{sppa}) and motor inhibition when applying stimulation at a wide range of intensities (***Figure 4A***), nor when testing the relationship between simulated intracranial intensities and changes in excitability (***Figure 4B***). Similarly, administration of a time-locked auditory masking stimulus that effectively reduced TUS detection rates (***Figure 7***) did not provide evidence of direct effects being obscured by audible differences between conditions (***Figure 6***). Taken together, this study presents no evidence for direct and spatially specific ultrasonic neuromodulation of motor excitability when applying a clearly audible 1000 Hz pulsed TUS protocol, despite using improved control conditions, higher stimulation intensities, and a larger sample size than prior studies (Fomenko et al., 2020; Legon, Bansal, et al., 2018; Xia et al., 2021). Building on these results, the current challenge is to develop efficacious neuromodulatory protocols with minimal auditory interference. Efforts in this direction are already underway (Mohammadjavadi et al., 2019; Nakajima et al., 2022; Zeng et al., 2022).

Sound-cued motor inhibition

Until now, it was unclear why or how TUS induced motor inhibition in humans. Here, we show that this inhibition is caused by peripheral auditory stimulation. It is well-known that MEPs are sensitive to both sensory and psychological factors (Duecker et al., 2013). For example, several studies find MEP attenuation following a startling auditory stimulus (Fisher et al., 2004; Furubayashi et al., 2000; Ilic et al., 2011; Kohn et al., 2004; Wessel & Aron, 2013), and have demonstrated the impact of stimulus duration and volume on this inhibition (Furubayashi et al., 2000). It is possible that a similar mechanism is at play for audible TUS protocols. Indeed, we observed modulation of motor cortical excitability dependent upon the characteristics of auditory stimuli, including their duration and timing (Experiment I: ***Figure 8***; Experiment III: ***Figure 9A***), their pitch/frequency (Experiment III: ***Figure 9B***), and whether the confound was audible in general, including perceived volume (Experiment II: ***Figure 4B***; Experiment IV: ***Figure 10***).

One possible interpretation of the observed MEP attenuation is that the auditory confound acts as a salient cue to predict the upcoming TMS pulse. Prediction-based attenuation has been reported in both sensory and motor domains (Ford et al., 2007; Tran et al., 2021a). For example, MEPs are suppressed when the timing of a TMS pulse can be predicted by a warning cue (Capozio et al., 2021; Tran et al., 2021a). In the current experimental setup, participants could also learn the relative timing of the auditory stimulus and the TMS pulse. Indeed, we observe MEP attenuation emerge across initial trials as participants learn when to expect TMS, until a stable (i.e., learned) state is reached (***Figure 11***). Moreover, no motor inhibition was observed when TUS onset was inaudible or when stimulation timing was potentially too fast to function as a predictive cue (100 ms). Taken together, a parsimonious explanation is that expectation-based inhibition drives motor inhibitory effects. This inhibitory response might either reflect inhibition of competing motor programs – a component of motor preparation – or a homeostatic process anticipating the TMS-induced excitation (Capozio et al., 2021; Tran et al., 2021a).

Considerations and future directions

Crucially, our results do not provide evidence that TUS is globally ineffective at inducing neuromodulation. While the present study and prior research highlight the confounding role of indirect auditory stimulation during pulsed TUS, there remains strong evidence for the efficacy of ultrasonic stimulation in animal work when auditory confounds are accounted for (Mohammadjavadi et al., 2019), or in controlled in-vitro systems such as an isolated retina, brain slices, or neuronal cultures in which the auditory confound carries no influence (Menz et al., 2013; Tyler et al., 2018).

The precise biomolecular and neurophysiological mechanisms of ultrasonic neuromodulation remain under rapidly progressing investigation (Weinreb & Moses, 2022; Yoo et al., 2022). Some theories focus on mechanical perturbation of neuronal lipid bilayer (El Hady & Machta, 2015; Heimburg & Jackson, 2005; Lemaire et al., 2019; Plaksin et al., 2014; Prieto et al., 2013), while others emphasize the role of mechanosensitive ion channels (Kubanek et al., 2018; Tyler et al., 2018). Regardless, the central role of acoustic radiation force is widely recognized, which could cause an increase in Ca^{2+} influx that prompts a signaling cascade ultimately triggering voltage-gated ion channels, leading to a modulation of action potentials (Yoo et al., 2022). Regardless of the exact mechanisms of action, a shared interpretation is that mechano-electrophysiological energy transfer is proportional to acoustic radiation force, and therefore also proportional to stimulation intensity.

Accordingly, in light with the abundant evidence from controlled systems, one could argue that the TUS dose in the present study could have been insufficient to evoke direct neuromodulation. Indeed, despite the applied intensities exceeding prior relevant human work (Fomenko et al., 2020; Legon, Bansal, et al., 2018; Xia et al., 2021) the total applied neuromodulatory doses are relatively low as compared to, for example, repetitive TUS protocols (rTUS) in animal work (Folloni et al., 2019; Verhagen et al., 2019) or recent human studies (Nakajima et al., 2022).

Alternatively, insufficient neural recruitment could perhaps be a consequence of other stimulation parameters besides intensity. If so, an absence of direct neuromodulation might not generalize to parameters outside the tested set. For example, while we replicated and extended prior work targeting the hand motor area at ~30 mm from the scalp (Fomenko et al., 2020; Legon, Bansal, et al., 2018; Xia et al., 2021), other studies have suggested that the optimal stimulation depth to engage the hand motor area may be more superficial (Osada et al., 2022; Siebner et al., 2022).

One might further argue that the TMS hotspot provides insufficient anatomical precision to appropriately target the underlying hand muscle representation with TUS. The motor hotspot may not precisely overly the cortical representation of the assessed muscle due to the increased coil-cortex distance introduced by the TUS transducer. This distance, and the larger TMS coils required to evoke consistent MEPs, results in a broad electric field that is substantially larger than the TUS beam width (e.g., 6 mm for 250 kHz; Fomenko et al., 2020; Legon, Bansal, et al., 2018). Moreover, given that the precise cortical site for TUS effects on corticospinal output is unknown, while for TMS the effects are likely evoked via the E-field produced in the crown or lip region of the precentral gyrus (Siebner et al., 2022), it is possible that a transducer aligned with the center of the TMS coil may not be adequate. Nevertheless, we note that previous work utilizing a similar targeting approach has effectively induced changes in corticospinal motor excitability (Zeng et al., 2022). We also note that our stimulation depth and targeting procedures were comparable to all prior TUS-TMS studies, and that our simulations confirmed targeting (***Figure 5A***).

The experimental conditions in the present study come with several limitations. First, the auditory stimuli used for sound-only sham and masking were administered at the same volume across participants (Experiments I-III), and while masking successfully blinded participants to stimulation, slight audible differences between on-target and active control sites persisted (Experiments I-II; ***Figure 7B***). Indeed, stimulation of the contralateral face representation as an active control site may not adequately match nonspecific peripheral stimulation. In contrast, stimulation of an inactive control site, the white matter ventromedial to the hand motor area, more closely replicates these peripheral effects, but the possibility of direct neuromodulation cannot be definitively excluded given evidence for white matter neuromodulation during deep brain stimulation in humans (Felix et al., 2022; Hamani et al., 2011; Lozano et al., 2008; Mayberg et al., 2005). Importantly, even when considering these potential limitations, we did not observe evidence for direct neuromodulation using either of these control sites, nor when using a sound-only sham condition. In summary, our main finding that the auditory confound drove motor inhibition in the present study, and likely had an impact in previous studies, holds true.

It follows that where an auditory confound could be expected, appropriate control conditions are critical. These controls could involve stimulating a control region, and/or inclusion of a matched sound-only sham. In parallel, or perhaps alternatively, the impact of this confound can be mitigated in several ways. First, we recommend that the influence of auditory components be considered in transducer design and selection. Second, masking the auditory confound can help to blind participants to experimental conditions. Titrating auditory mask quality by participant to account for intra- and

inter-individual differences in subjective perception of the auditory confound would be beneficial. However, this auditory stimulation might still influence cognitive task performance, among other measures. Third, the ultrasonic pulse and pulse train can be modulated, or ramped, to minimize or even eliminate the auditory confound. This approach still requires validation and will only be relevant for protocols with pulses of sufficient duration (e.g., longer than 20 ms). Here, one can expect that the experimental control required to account for auditory confounds might also hold for alternative peripheral effects, such as somatosensory confounds. Longer pulse durations are common in offline rTUS paradigms (Zeng et al., 2022), with more opportunity for inaudible pulse shaping and the added benefit of separating the time of stimulation from that of measurement. However, appropriate control conditions remain central to make inferences on interventional specificity.

Conclusion

Transcranial ultrasonic stimulation is rapidly gaining traction as a promising neuromodulatory technique in humans. For TUS to reach its full potential we must identify robust and effective stimulation protocols. Here, we demonstrate that one of the most reliable findings in the human literature – online motor cortical inhibition during a 1000 Hz pulsed protocol – primarily stems from an auditory confound rather than direct neuromodulation. Future research must carefully account for peripheral confounding factors to isolate direct neuromodulatory effects of TUS, thereby enabling the swift and successful implementation of this technology in both research and clinical settings.

Methods

Overview of experiments

In four experiments conducted across three institutions, we investigated the role of the auditory confound in a combined TUS-TMS paradigm. We employed tightly matched control conditions to disentangle direct neuromodulatory effects of TUS from those driven by the salient auditory confound associated with a 1000 Hz pulsed protocol.

In Experiments I and II, we tested for a spatially specific and direct effect of TUS by applying on-target stimulation over the left-hemispheric hand motor area and active control stimulation over the right-hemispheric face motor area. Further, we employed a sound-sham condition where only auditory stimulation was delivered. In these experiments, we additionally tested for a dose-response relationship between modulation of motor cortical excitability and spatial-peak pulse-average intensity (I_{sppa}). Here, we also investigated the relationship between simulated intracranial I_{sppa} and changes in MEP amplitude. We accounted for potential audible differences between stimulation sites using an auditory masking stimulus time-locked to ultrasonic stimulation and assessed its efficacy. Finally, in Experiment I we tested for a stimulus duration dependent effect of TUS on motor excitability. Experiment II has been preregistered to confirm and extend the findings of Experiment I (https://doi.org/10.17605/OSF.IO/HS8PT).

In Experiment III, we interrogated the role of auditory characteristics on motor excitability and tested for a direct neuromodulatory effect of TUS by administering auditory stimuli of varying duration and pitch, both with and without ultrasonic stimulation.

In Experiment IV, we aimed to distill the effects of auditory confound volume and applied TUS to an inactive control site – the white matter ventromedial to the hand motor area – at three intensities. To further probe the role of TUS audibility (e.g., of on- and offset) in modulation of motor cortical excitability we administered stimulation both with and without a continuous masking stimulus. See ***Figure 1*** for an overview.

Experiment I & Experiment II

Participants and sessions

We investigated the effect of TUS on motor excitability across two experiments. In Experiment I, 14 participants were recruited (6 female; M_{age} = 25.9, SD_{age} = 4.6). In Experiment II, 31 participants were recruited (15 female; M_{age} = 24.1, SD_{age} = 3.7). Participants were primarily students recruited from the Radboud University SONA research platform. All included participants were healthy and right-handed. Participants underwent screening for contraindications to non-invasive brain stimulation, including for any history of psychiatric or neurological disorders and the use of medications that may influence brain excitability. All participants provided informed consent. These same criteria were met across all four experiments. In Experiment I, two participants were excluded, one where a baseline measurement was disrupted and thus missing, and another in whom the required TMS intensity to elicit a ~1 mV MEP was beyond range, likely as a result of the increased coil-scalp distance necessitated by the TUS transducer positioning. In Experiment II, four participants were excluded in total, where two participants required a TMS intensity that was beyond range and one participant did not meet inclusion criteria for the brain stimulation session. Participation was terminated for a fourth

participant who experienced vasovagal syncope during the beginning of TMS hotspot localization. No TUS was administered to this participant.

Participants completed two sessions, the first involving an MRI scan used for online neuronavigation and post-hoc acoustic and thermal simulations, and the second involving transcranial ultrasonic and magnetic stimulation. The local ethics committee approved both experiments (CMO/METC Arnhem-Nijmegen: protocol NL76920.091.21 [Experiment I] and protocol NL80331.091.22 [Experiment II]). Both experiments were conducted in accordance with the Declaration of Helsinki.

MRI

Each participant underwent an MRI scan for the purposes of online neuronavigation and post-hoc simulations of ultrasonic stimulation. These scans were performed at the Donders Centre for Cognitive Neuroimaging on a 3T Siemens Skyra MRI scanner (Siemens Medical Solutions, Erlangen, Germany) using a 32-channel head coil. The following parameters were used for T1-weighted anatomical scans: TR = 2700 ms, TE = 3.69 ms, FoV read = 230 mm, FoV phase = 128.1%, slice thickness = 0.9 mm, number of slices = 224. T2-weighted anatomical scans were acquired to support MR-based skull segmentation at the following parameters: TR = 3200 ms, TE = 408 ms, FoV read = 230 mm, FoV phase = 128.1%, slice thickness = 0.9 mm, number of slices = 224.

Transcranial ultrasonic stimulation

We delivered ultrasonic stimulation with the NeuroFUS system (manufacturer: Sonic Concepts Inc., Bothell, WA, USA; supplier/support: Brainbox Ltd., Cardiff, UK) using two piezoelectric ultrasound transducers, one to stimulate the left-hemispheric hand motor area (on-target TUS) and one to stimulate the right-hemispheric face motor area (active control TUS). Each transducer consisted of a two-element annular array with solid water coupling. A radiofrequency amplifier powered both transducers via a matching network (Transducer Power Output system; manufacturer: Sonic Concepts Inc., Bothell, WA, USA; supplier/support: Brainbox Ltd., Cardiff, UK). Ultrasound gel was used to couple the transducers to the participant's scalp (Aquasonic 100, Parker Laboratories, NJ, USA).

In Experiment I, on-target TUS was administered with a 500 kHz fundamental frequency transducer (CTX500-06) at its minimum sonication depth of 35.1 mm. Active control TUS was administered with a 250 kHz transducer (CTX250-09) at the same depth. In Experiment II, to facilitate transcranial energy transmission and to stimulate a greater area, on-target TUS was instead administered with a 250 kHz transducer (CTX250-014) at a sonication depth of 28 mm. All transducers had a diameter of 45 mm and a width of ~16 mm.

Ultrasonic stimulation parameters for these experiments were chosen to match those of previous combined online TUS-TMS research where possible. The following parameters were used (***Figure 12A***): pulse duration (PD) = 0.3 ms; pulse repetition period (PRP) = 1 ms; pulse repetition frequency (PRF) = 1000 Hz; duty cycle (DC) = 30%; pulse shape: rectangular. In Experiment I, TUS was applied at 100 and 500 ms stimulus durations, and at both 32.5 and 65 W/cm^2 spatial-peak pulse-average intensities in free-water (I_{sppa}) to the hand motor area, corresponding to pressures of 1.44 and 1.02 MPa, and spatial-peak temporal-average intensities (I_{spta}) of 9.75 and 19.50 W/cm^2. In Experiment II, TUS was applied for a 500 ms stimulus duration only, at both 6.35 and 19.06 W/cm^2 I_{sppa},

corresponding to pressures of 0.45 and 0.78 MPa, and an I_{spta} of 1.9 and 5.7 W/cm^2. All stimulation intensities reported are as quantified by the manufacturer in free-water unless explicitly stated otherwise, i.e., these are stimulation output intensities without attenuation from biological tissue. Estimated intracranial intensities are reported in the Results section, ***Figures 4*** and ***5***.

Concurrent TUS-TMS

We combined TUS and TMS to investigate the effect of ultrasonic stimulation on motor cortical excitability. Prior research has demonstrated that ultrasonic stimulation does not affect the electromagnetic field produced by TMS, nor does TMS affect the pressure field resulting from ultrasonic stimulation (Legon, Bansal, et al., 2018; Xia et al., 2021).

Single-pulse TMS was delivered with a 97 mm figure-of-eight MC-B70 coil powered by a MagPro X100 + MagOption stimulator (MagVenture, Farum, Denmark). The coil was held at a 45° angle from midline to induce an approximate posterolateral to anteromedial current between the peak to trough of the applied biphasic pulse shape. The motor hotspot for the first dorsal interosseous (FDI) was determined by positioning the TMS coil over the hand motor area as identified with neuronavigation software, and iteratively adjusting TMS intensity until a consistent MEP was observed around 1mV of amplitude. After probing locations in a ~2 cm radius, the location resulting in the highest and most stable amplitude MEPs was set as the final stimulation site. The percentage of maximum stimulator output was adjusted until an average MEP amplitude of ~1 mV was observed across approximately ten trials. This intensity was used throughout the rest of the experiment. The mean percentage of administered maximum stimulator output was 80.4 ± 12.5% for Experiment I, and 88.0 ± 9.3% for Experiment II. These high stimulation intensities are to be expected, given the offset of TMS from the scalp owing to the ultrasound transducer and the TMS current dissipating with distance (O'Shea & Walsh, 2007).

To apply TUS and TMS concurrently, the ultrasound transducer was affixed to the center of the TMS coil using a custom-made 3D-printed clamp (***Figure 12B***; DOI: 10.5281/zenodo.6517599). A ~2 mm thick layer of neoprene was placed between the TUS-TMS clamp and the TMS coil to prevent the formation of a sound chamber resulting in substantially louder TMS clicks. To administer stimulation at high temporal precision, both TUS and TMS were externally triggered using Signal version 7.05 (CED, Cambridge, UK), where TMS was consistently applied 10 ms prior to the offset of ultrasound. This same software was used to update ultrasonic stimulation parameters via serial commands between trials.

Neuronavigation

We used online neuronavigation to support target selection and consistent TMS and TUS placement. To this end, individual T1-weighted scans were loaded in the Localite neuronavigation system (Localite Biomedical Visualization Systems GmbH, Sankt Augustin, Germany), with the exception of two participants in Experiment I for whom standard MNI templates were used due to inaccessibility of their individual MRI scans in time for the second session. The hand area of the primary motor cortex was then identified based on the anatomical scan for each subject to support the identification of the TMS hotspot. An infrared stereo-optical tracking camera (Polaris Spectra, Northern Digital Inc., Waterloo, Ontario, Canada) captured the location of two trackers that consisted of three spherical fiducial markers affixed to participant's forehead and the TMS coil. We recorded the location of TMS during the experiment, and by extension on-target TUS over the hand area, for post-hoc simulations.

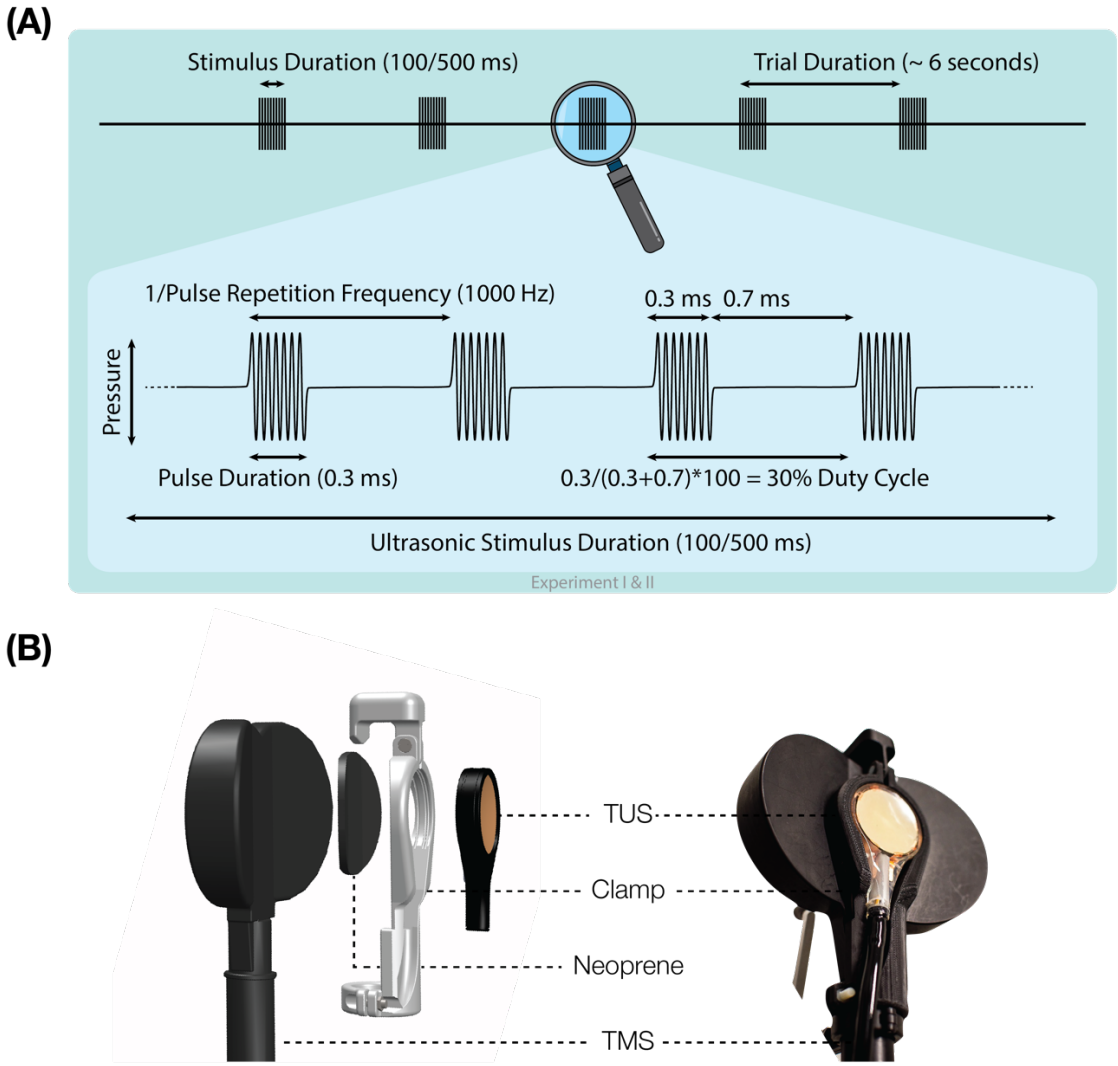

Figure 12. Ultrasonic stimulation parameters and TUS-TMS setup for Experiments I and II. (A) Stimulus duration = 100 ms [Experiment I]/500 ms [Experiments I & II]; trial duration = 6 ± 1 s; pulse repetition frequency = 1000 Hz, pulse duration = 0.3 ms; duty cycle = 30%; pulse shape: rectangular (no explicit ramping or smoothing). For Experiment III, pulse duration = 0.1 ms, and duty cycle = 10%. For Experiment IV, stimulus duration = 400 ms. **(B)** TUS-TMS clamp (DOI: 10.5281/zenodo.6517599).

Electromyography

Muscular activity in the FDI was recorded via electromyography (EMG) with surface adhesive electrodes using a belly-tendon montage with the reference electrode placed on the middle phalanx of the right index finger. The EMG signal was amplified with a 1000-fold gain, bandpass filtered in a 1Hz-1kHz range (D440-2, Digitimer Ltd., Hertfordshire, UK), and digitally sampled at 5 kHz (Micro 1401, CED, Cambridge, UK). Signal version 7.05 controlled the acquisition and stored the data for offline analysis (CED, Cambridge, UK).

Experimental conditions

To determine the effect of TUS on motor cortical excitability, on-target stimulation was applied over the left-hemispheric hand area in the primary motor cortex. To assess specificity and account for auditory and potential somatosensory confounds, we included active control and sound-only sham conditions (***Figure 13A***; Airan & Butts Pauly, 2018; Braun et al., 2020; Guo et al., 2018; Sato et al., 2018).

The active control condition served to account for peripheral confounds, albeit over a different region, and to demonstrate the spatial specificity of ultrasonic neuromodulation. This control consisted of stimulating the face representation in the contralateral (i.e., right-hemispheric) primary motor cortex. We elected for the right-hemispheric face area given its relatively analogous location and the absence of direct interhemispheric connections to the left-hemispheric hand area (Schmahmann & Pandya, 2006). The observation that ultrasonic stimulation of the hand area does not alter contralateral hand motor area excitability further supports our choice for this control region (Ai et al., 2018; Xia et al., 2021). We used neuronavigation to target the right-hemispheric face area at the start of the session and held this position during the experiment. Active control stimulation was applied at identical stimulation parameters to on-target stimulation (see *transcranial ultrasonic stimulation*) in Experiment II. In Experiment I, however, a 500 kHz transducer delivered on-target stimulation while a 250 kHz transducer delivered active control stimulation, due to practical and technical constraints. Upon recalibration of these transducers, the applied intensities in Experiment I for the active control condition differed from on-target stimulation, at 7.20 and 14.53 W/cm^2 I_{sppa} in free-water, corresponding to pressures of 0.48 and 0.68 MPa, and an I_{spta} of 2.19 and 4.35 W/cm^2.

The sound-sham condition controlled for the auditory confound accompanying TUS and allowed for quantification of any generalized effect of stimulation. During this condition we did not administer any ultrasonic stimulation, but instead played an auditory stimulus over headphones. The auditory stimulus consisted of a MATLAB-generated 1000 Hz square wave to mimic the audible 1000 Hz PRF of TUS, with additional white noise added at a signal-to-noise ratio of 4:1. In Experiment I, the auditory stimulus was played over bone conducting headphones (AfterShockz Trekz, TX, USA) to closely mimic the mode of entry of the auditory confound (Braun et al., 2020). However, due to Bluetooth signal delays, the length of this tone exceeded that of the corresponding ultrasonic stimulus duration by 100 ms (i.e., tone duration = 200/600 ms), where the tone began approximately 50 ms before TUS. In Experiment II, in-ear headphones were used to present the sound-sham condition with millisecond precise timing (i.e., 500 ms; ER-3C Insert Earphones, Etymotic Research, Illinois, USA).

With consideration of potentially audible differences between on-target and active control TUS, we applied these conditions both with and without masking stimuli identical to the auditory stimuli used for the sound-sham condition (***Figure 13B***, Braun et al., 2020).

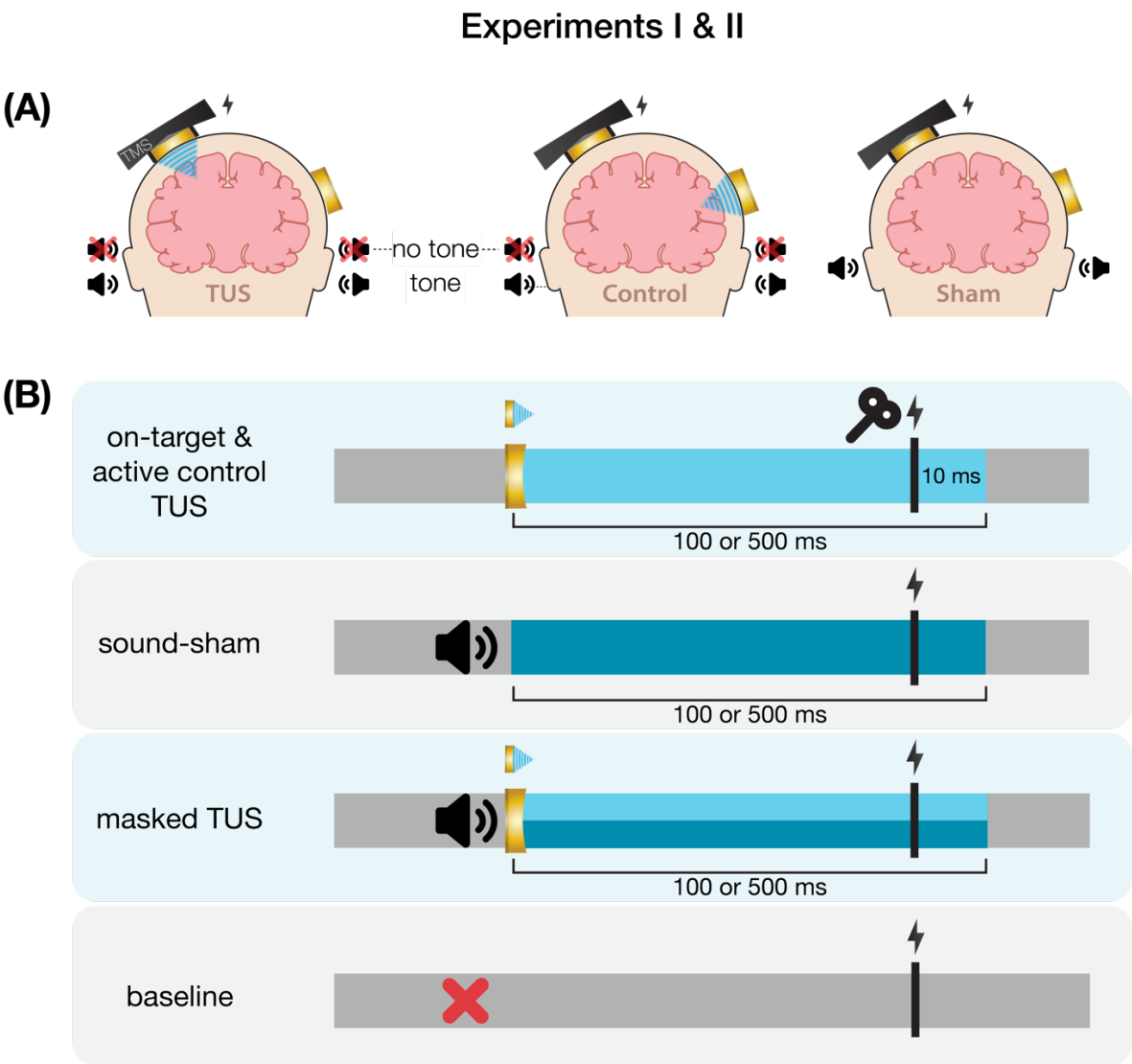

Figure 13. Conditions and timing of Experiments I and II. (A) On-target left-hemispheric hand area stimulation (left) and active control right-hemispheric face area stimulation (middle) were applied both with and without a masking tone. The sham condition (right) consisted solely of an identical tone. **(B)** On-target and active control TUS were administered for 100 ms [Experiment I] and 500 ms [Experiments I & II] with TMS applied 10 ms prior to TUS-offset. In Experiment I, the auditory stimulus administered during sound-sham and masked conditions began ~50 earlier and was 100 ms longer than TUS, while in Experiment II the auditory stimulus was precisely timed to match TUS. Baseline measurement involved no intervention other than TMS.

Experiment I

In Experiment I, participants underwent three main conditions: on-target TUS, active control TUS, and sound-sham, as well as a baseline condition. In this experiment, TUS was administered at both 100 and 500 ms stimulus durations to probe the previously reported stimulus duration dependent inhibition of motor excitability (Fomenko et al., 2020). On-target and active control conditions were presented both with and without an auditory masking stimulus to account for potential audible differences between stimulation sites. For 500 ms stimulus durations, ultrasonic stimulation was applied at both 32.5 and 65 W/cm^2 I_{sppa} to investigate a dose-response relationship with motor inhibition.

We administered conditions in a single-blind inter-subject counterbalanced blocked design. Prior research indicates that larger effect sizes may be observed in a blocked rather than interleaved protocol, particularly at a duty cycle of 30% (Fomenko et al., 2020; Xia et al., 2021). During the experiment, participants received stimulation at rest while looking at a fixation cross presented on a monitor.

In total, participants completed 14 blocks of 20 trials each, matching the recommended number of trials to obtain reliable measurements of excitability (Biabani et al., 2018; Goldsworthy et al., 2016). Two baseline measurements were completed, the first occurring as one of the first four blocks, and the second as one of the last four, to capture any general shift in excitability throughout the experiment. Following each block, the participant was given a 15 second break. Following the fifth and eighth block, the participant was given a break for a few minutes. Each trial lasted 6 ± 1 seconds. TMS was administered on every trial for a total of 280 single pulses. TMS was time-locked to occur 10 ms prior to the offset of TUS, i.e., after 90 and 490 ms of ultrasonic stimulation for 100 and 500 ms stimulus durations respectively (***Figure 13B***). In the sound-sham condition, and when TUS was masked, the auditory stimulus began ~50 ms earlier.

Experiment II

To confirm and expand upon our findings from Experiment I, we conducted a second experiment using the same main conditions and procedures, with a few adaptations. The design was 2x2x2 comprising of stimulation site (on-target/active control), stimulation intensity (6.35/19.05 W/cm^2), and auditory masking (no mask/masked). In addition, participants underwent a baseline condition (i.e., TMS-only) and a sound-sham condition where only an auditory stimulus was delivered. We applied ultrasonic stimulation exclusively at an effective 500 ms stimulus duration, and the auditory stimulus used for masking and sound-sham was 500 ms, precisely timed in concurrence with TUS, and delivered over insert earphones.

To better capture any baseline shift in excitability during the experiment, we presented conditions in a single-blind pseudorandomized order in which each consecutive set of 10 trials included each of 10 conditions once. Participants completed 25 trials per condition, resulting in 250 trials total. Every 20 trials the participant received a 15 second break, and after 80 and 160 trials, the participants received a break of a few minutes.

Masking assessment

To gauge the efficacy of our masking stimulus to blind participants to TUS, we conducted an additional masking assessment for Experiment II. Here, we tested how well participants could determine whether they had received ultrasonic stimulation across each condition, excluding baseline. Participants completed 4 trials per condition, resulting in 36 trials in total, presented in a pseudorandomized order where each condition is presented randomly in sets of 9 trials.

It is possible that the masking stimulus effectively blinds participants to whether they have received TUS, but that audible differences remain between on-target and active control sites. To test for audible differences between stimulation sites, participants were exposed to two subsequent masked TUS trials. These two stimuli were either the same (i.e., [on-target + on-target] or [active control + active control]) or different (i.e., [on-target + active-control/active-control + on-target]).

These two trials were presented at both intensities (6.35 and 19.05 W/cm^2), to account for the louder auditory confound associated with higher intensity stimulation. Following each pair of trials, participants were asked to rate their similarity on a visual analog scale (0 = very dissimilar, 100 = very similar) across 8 trials in total.

Simulations

To obtain estimates of acoustic targeting, realized intracranial dosage, and safety indices, we conducted individualized 3D simulations of acoustic and thermal effects for Experiments I and II using the validated k-Wave MATLAB toolbox, a pseudospectral time-domain solver (Treeby & Cox, 2010).

Preprocessing was performed in MATLAB 2019b. Anatomical scans (T1w and T2w) were first segmented into distinct tissues using the SimNIBS headreco tool (Thielscher et al., 2015). We then reoriented the segmented volumes such that the axial plane of the recorded transducer location was parallel to the cartesian axis of the computational grid. Subsequently, the segmented volumes were resampled to an isometric volume size of 0.5 mm and interpolated using the nearest neighbor algorithm. We then extracted the skull, scalp, and brain – including gray and white matter – volumes. To correct minor segmentation errors, the volumes were smoothed by a cubic averaging kernel using a window size of 4 voxels, and re-binarized. The skull layer was additionally combined with a one-voxel outer layer of the filled-in bone volume provided by SimNIBS. Any gaps between skull and skin volumes were assigned to the skull. The skull, scalp, and brain were all included in acoustic and thermal k-Wave simulations, where all voxels not assigned to these tissues were designated as water. Segmented volumes were then cropped to include the whole skull and the transducer, including a perfectly matched layer (PML) of 10 grid points. The points per wavelength given the 0.5 mm grid spacing was 6 for Experiment I (f = 500 kHz) and 12 for Experiment II (f = 250 kHz).

The acoustic properties of sound speed, density, alpha coefficient, and alpha power, as well as the thermal properties of thermal conductivity and heat capacity, were assigned to the skull, scalp, and brain, as reported in ***Table 1*** (Aubry et al., 2022; Hasgall et al., 2022).

We modelled on-target TUS with two-element annular arrays using their respective geometric dimensions and fundamental frequencies for Experiments I and II. The position and orientation of the simulated transducer was extrapolated based on the coordinates of the TMS coil recorded during the experiment with neuronavigation software. We calibrated the simulated source amplitude and phase in free-water to reach the applied free-water stimulation intensities of 32.5 and 65 W/cm^2 (Experiment I) and 6.35 and 19.06 W/cm^2 (Experiment II). We calibrated the simulated transducer such that the center of the acoustic profile's full-length half-maximum was at the applied depths of 35.1 mm (Experiment I) and 28 mm (Experiment II) from the exit plane of the transducer. The source amplitude and phase resulting in a simulated acoustic profile with the minimum error in relation to the water-tank calibrated acoustic profile provided by the manufacturer were used for acoustic and thermal simulations including the tissue volumes.

Acoustic simulations were then run for three TUS cycles after reaching the steady-state pressure distribution per applied free-water intensity per participant. The maximum pressure map computed by k-Wave was then used to calculate the realized intracranial pulse-average intensity, which was calculated as: $I_{pa} = \frac{p^2}{2c\rho}$, where p is acoustic pressure, c is sound speed, and ρ is density. The mechanical index was calculated based on simulated intracranial pressure as: $MI = \frac{p}{\sqrt{f}}$, where p

is the peak intracranial pressure, and *f* is the fundamental frequency. This pressure map further served as input for the thermal simulations, where we quantified the maximum thermal rise at each point in the computation grid. Here, simulations were run with a 30% DC for a stimulus duration of 500 ms, corresponding to the applied TUS. To compute a conservative safety estimate of thermal rise, stimulation was split into five 100 ms steps, each with a 30 ms on-period and a 70 ms off-period (actual on-period = 0.3 ms per 1 ms).

Table 1. Acoustic properties.

	Density (kg/m^3)	Sound speed (ms)	Attenuation coefficient	Thermal conductivity (W/m/°C)	Specific heat capacity (J/kg/°C)
Water	994	1500	0.0	0.60	4178
Scalp	1090	1610	0.4	0.37	3391
Skull	1850	2800	8.0	0.32	1313
Brain	1046	1546	0.6	0.51	3630

Analysis

We exported EMG data from Signal 7.05 (CED, Cambridge, UK) to MATLAB, where MEP peak-to-peak amplitude was calculated using a custom MATLAB script and confirmed by trial-level visual inspection. Trials where noise prevented an MEP to be sufficiently quantified were removed. Given the right-skewed nature of the raw MEP values, we performed a square root transformation to support parametric statistics. For visualization purposes, baseline corrected MEP amplitudes were also calculated.

Linear mixed-effects models (LMMs) were fitted using the lme4 package in R (Bates et al., 2015; R core team, 2021). Intercepts and condition differences (slopes) were allowed to vary across participants, including all possible random intercepts, slopes, and correlations in a maximal random effects structure (Barr et al., 2013). Statistical significance was set at two-tailed $\alpha = 0.05$ and was computed with t-tests using the Satterthwaite approximation of degrees of freedom. For direct comparisons to a reference level (e.g., baseline), we report the intercept (*b*), standard error (*SE*), test-statistic (*t*), and significance (*p*). For main effects and interactions, we report the F statistic, significance, and partial eta squared. LMMs included square root transformed MEP peak-to-peak amplitude as the dependent variable, with the relevant experimental conditions and their interactions as predictors.

To investigate a dose-response relationship for simulated intensities, square root corrected MEP amplitude was expressed as a percentage of baseline, active control, and sound-sham conditions. For each of these dependent variables, a simple linear model was run predicting percentage change by simulated intracranial intensity, for the two free-water stimulation intensities separately. This analysis was only conducted for Experiment II, as the sample size of Experiment I was not sufficient.

To assess whether masking effectively blinded participants to stimulation, we used a mixed effects logistic regression to predict participant response (stimulation yes/no) as a function of stimulation site (on-target/active control), free-water intensity (6.35 and 19.05 W/cm^2), and masking (no mask/masked) with a random intercept by participant.

Finally, to determine whether audible differences between on-target and active control stimulation might be present even during auditory masking, we conducted a two-way repeated measures ANOVA predicting similarity rating by stimulation site (same/different) and stimulation intensity.

Experiment III

Participants

We further characterized the effect of auditory confounds on motor cortical excitability in Experiment III by administering auditory stimuli of varied pitch and duration, both with and without ultrasonic stimulation of the hand motor area. To this end, 16 participants were recruited (8 female; M_{age} = 31.4, SD_{age} = 7.9). No participants were excluded. Inclusion criteria and ethical procedures are as in Experiments I & II. Ethical approval was obtained from the local Toronto University Health Network Research Ethics Board (approval code: 20-5740).

Transcranial ultrasonic stimulation

We delivered ultrasonic stimulation with the NeuroFUS system (manufacturer: Sonic Concepts Inc., Bothell, WA, USA; supplier/support: Brainbox Ltd., Cardiff, UK) using a custom piezoelectric ultrasound transducer consisting of a two-element annular array without 'solid water coupling'. A radiofrequency amplifier powered the transducer via a matching network (Transducer Power Output system; manufacturer: Sonic Concepts Inc., Bothell, WA, USA; supplier/support: Brainbox Ltd., Cardiff, UK). The transducer (H246-01) had a diameter of 38 mm, a width of 10 mm, and operated at a fundamental frequency of 500 kHz with a sonication depth of 30 mm. Ultrasound gel (Wavelength MP Blue Multi-Purpose Ultra-sound Gel, Sabel Med, Oldsmar, FL) and a 1.5 mm thick gel-pad (Aquaflex, Parker Laboratories, NJ, USA) were used to couple the transducer to the participants' scalp. Please note, the auditory confound originating from the transducer used in Experiment III might have a different pitch, timbre, and sound volume than the auditory confound originating from the transducers in Experiments I, II, and IV. This is the case even when using exactly the same stimulation parameters, and is caused by differences in the physical characteristics of the transducers, including the presence or absence of an additional solid coupling layer.

Ultrasonic stimulation parameters for this experiment were largely identical to those used in Experiments I & II, and prior combined TUS-TMS studies (***Figure 12A***; Fomenko et al., 2020; Legon et al., 2018; Xia et al., 2021), namely using a 1000 Hz PRF with a 500 ms stimulus duration. Here, TUS was applied at a 10% DC (i.e., a 0.1 ms PD) at 9.26 W/cm^2 free-water I_{sppa}, corresponding to a pressure of 0.54 MPa, and an I_{spta} of 0.93 W/cm^2. The 0.3 dB/cm-MHz derated mechanical index for this protocol is 0.47.

Concurrent TUS-TMS

Single-pulse TMS was delivered via a 70 mm figure-of-eight coil powered by a Magstim 200^2 stimulator (Magstim, Whitland, Dyfed, UK). The coil was held at 45° from midline to induce an approximate posterolateral to anteromedial using a monophasic pulse shape. Optimal positioning was determined by placing the TMS coil over the left-hemispheric hand motor area and moving the coil in increments

of 0.5 cm until a clear MEP was observed over the FDI. Following assessment of optimal coil flatness and orientation, the location and orientation of TMS were marked on the scalp to support consistent placement throughout the experiment. At this site, the minimal intensity required to evoke an average MEP of ~1 mV across ten trials was determined.

The ultrasound transducer was affixed to the center of the TMS coil using a custom 3D-printed clamp as described in a previously published study (Fomenko et al., 2020). To administer stimulation at high temporal precision, both TUS and TMS were externally triggered using Signal 6.04 (CED, Cambridge, UK), where TMS was consistently applied 10 ms prior to the offset of ultrasound.

Electromyography

Muscular activity in the FDI was recorded via EMG. The signal was amplified with a 1000-fold gain (Intronix Technologies Corporation [model: 2024F], Bolton, Canada), bandpass filtered (20 Hz – 2.5 kHz) and digitally sampled at 5 kHz (Micro1401; CED, Cambridge, UK). Signal version 6.04 (CED, Cambridge, UK) stored data for offline analysis.

Experimental conditions and procedures

Experiment III comprised of two parts. In Part I, we directly assessed changes in motor excitability from baseline following four different sound-only sham conditions, varying in pitch and duration. In Part II, we assessed whether applying TUS over the hand motor area during the presentation of these auditory stimuli further affected motor excitability (***Figure 14A***).

Auditory stimuli were presented at two pitches. A 1 kHz tone was administered as in Experiments I, II, IV, and previous research (Braun et al., 2020). This stimulus was delivered over noise-cancelling earbuds. In addition, a 12 kHz tone was administered as in prior research by Fomenko and colleagues (2020). This tone was selected to match the auditory confound originating from this specific transducer. This stimulus was delivered via speakers positioned to the left of the participant. The auditory stimuli were either 500 ms in duration, precisely time-locked to when ultrasonic stimulation was administered, or 700 ms in duration enveloping ultrasonic stimulation (i.e., starting 100 ms prior and ending 100 ms after TUS; ***Figure 14B***).

In Part I, TMS intensity was set to evoke a ~1 mV MEP in the absence of any auditory or ultrasonic stimuli, but with the ultrasound transducer affixed to the TMS coil. The mean percentage of maximum stimulator output was 73.7 ± 11.1%. Participants then received 15 trials of baseline measurement (i.e., TMS only), and 15 trials of each of the four auditory stimuli. Conditions were presented in blocks in a single-blind randomized order.

In Part II, TMS intensity was set to evoke a ~1 mV MEP separately for each of the four sound-only sham conditions: 77.4 ± 9.4% [1 kHz, 500 ms], 77.6 ± 10.1% [1 kHz, 700 ms], 76.9 ± 10.6% [12 kHz, 500 ms], and 77.2 ± 9.8% [12 kHz, 700 ms]. Participants then received 15 trials of each auditory stimulus, once with TUS applied to the hand motor area and once without TUS (i.e., sound-sham). Conditions were presented in pairs of sound-sham and TUS for each auditory stimulus. The order of sound-sham and TUS for a given pair was counterbalanced between subjects, and the order of the different auditory stimuli was randomized across participants.

Throughout the experiment, an inter-trial interval of 5 seconds was used. Participants were seated comfortably in a chair with a pillow placed beneath their arms, with MEPs being recorded at rest.

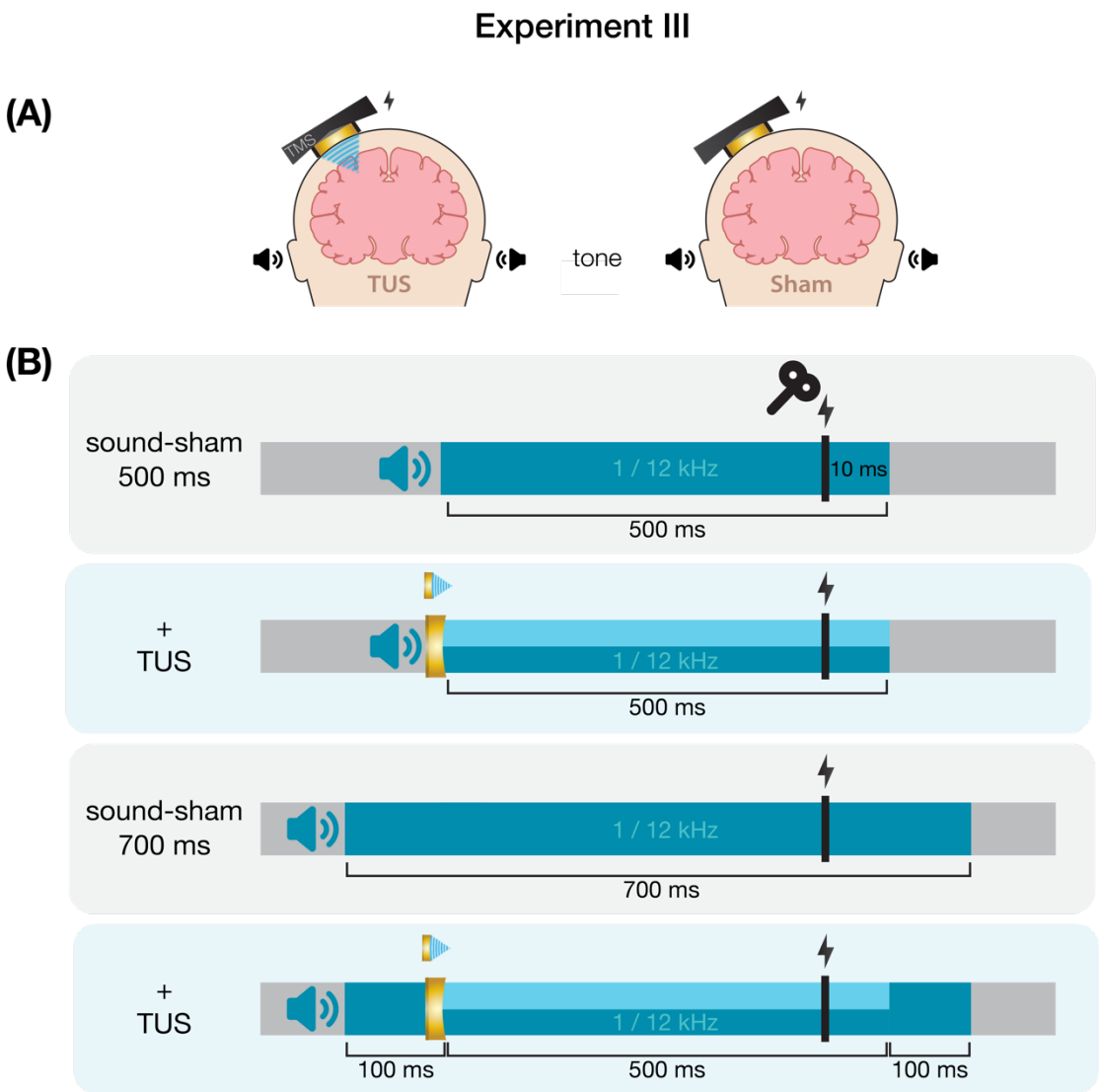

Figure 14. Conditions and timing of Experiment III. (A) On-target TUS consisted of left-hemispheric hand motor area stimulation in concurrence with an auditory stimulus (left), while sound-sham consisted solely of an auditory stimulus (right). **(B)** Auditory stimuli were delivered for either 500 or 700 ms. TUS was delivered for 500 ms. TMS was delivered 10 ms prior to TUS offset (i.e., following 490 ms of TUS), and at the same timing in the absence of TUS.

Analysis

Data preprocessing and LMMs with a maximal random effects structure (Barr et al., 2013) were conducted using the same conventions as Experiments I and II. In one subject, the 1 kHz, 700 ms TUS condition (Part II) was missing due to technical problems.

In this experiment, TUS was solely administered in Part II, while baseline measurements were solely made in Part I. In Experiments I and II, on-target TUS was directly compared to baseline. To make the same comparison for this experiment, we accounted for the different TMS intensities required to evoke a 1 mV MEP for baseline measurements in Part I and the TMS intensities required for the sound-sham conditions in Part II (***Supplementary Figure 6***). The *Relative MEP Amplitude* was calculated by dividing the TMS intensity required for baseline by the TMS intensity administered on each trial and multiplying square root corrected MEP amplitude by this correction factor.

Experiment IV

Participants

We recruited sixteen participants to further investigate the role of TUS audibility on motor excitability (15 female; M_{age} = 23.0, SD_{age} = 2.7). Two participants were excluded where the required TMS intensity was beyond range, and an additional two following technical difficulties, leaving twelve complete datasets for analysis. Inclusion criteria and ethical procedures are as in Experiments I & II. Ethical approval was obtained from the Ethics Committee of the Landesärztekammer Rheinland-Pfalz (2021-15808_01).

MRI

Each participant underwent an MRI scan for the purposes of online neuronavigation. These scans were performed at the Neuroimaging Center (NIC) of the Johannes Gutenberg University Medical Center Mainz on a 3T Siemens Prisma MRI scanner using a 32-channel head coil. The following parameters were used for T1-weighted anatomical scans: TR = 2700 ms, TE = 3.7 ms, FoV read = 260 mm, FoV phase = 88.9%, slice thickness = 0.9 mm, number of slices = 224.

Transcranial ultrasonic stimulation

We delivered ultrasonic stimulation with the NeuroFUS system (manufacturer: Sonic Concepts Inc., Bothell, WA, USA; supplier/support: Brainbox Ltd., Cardiff, UK) using an ultrasound transducer consisting of a two-element annular array with solid water coupling. A radiofrequency amplifier powered the transducer via a matching network (Transducer Power Output system; manufacturer: Sonic Concepts Inc., Bothell, WA, USA; supplier/support: Brainbox Ltd., Cardiff, UK). The transducer (CTX250-05) had an active diameter of 45 mm, a width of 16.45 mm, and operated at a fundamental frequency of 250 kHz using a sonication depth of 50 mm. Ultrasound gel (Aquasonic 100, Parker Laboratories, NJ, USA) and a ~2-3 mm thick gel-pad were used to couple the transducer to the participant's scalp (Aquaflex, Parker Laboratories, NJ, USA).

Ultrasonic stimulation parameters for this experiment were largely identical to those used in Experiments I & II and prior combined TUS-TMS studies (***Figure 2A;*** Fomenko et al., 2020; Legon et al., 2018; Xia et al., 2021), namely using a 1000 Hz PRF with a 30% DC. Here, TUS was consistently applied for a 400 ms stimulus duration at three free-water intensities: 4.34, 8.69, and 10.52 W/cm^2 I_{sppa}, corresponding to 0.37, 0.53, and 0.58 MPa, and 1.30, 2.61, and 3.16 W/cm^2 I_{spta}. The 0.3 dB/cm-MHz derated mechanical indices are 0.53, 0.76, and 0.83. In contrast to Experiments I and II, these intensities are applied to an inactive site to investigate auditory confound volume, rather than a dose-response relationship with on-target TUS.

Concurrent TUS-TMS

The TMS stimulator, coil, pulse shape, and orientation were identical to Experiments I & II, excluding the final four participants in which the Cool-B35 HO coil (Magventure, Farum, Denmark) was used

during preparatory measures to allow more precise estimation of the motor hotspot, while always the same TMS coil (MC-B70) was used during the combined TUS-TMS experiment.

The motor hotspot for the abductor pollicis brevis (APB) was determined by positioning the TMS coil over the hand motor area as identified with neuronavigation software, and systematically searching for the largest and most consistent MEP. An automated adaptive staircase procedure, with an amplitude threshold of 0.05 mV was used to determine the resting motor threshold (rMT). We subsequently estimated the dose response curve by applying 20 pulses each at 80, 90, 100, 110, 120, and 130% rMT. In most cases we were unable to reach the plateau of the dose-response curve due to the high motor thresholds resulting from the offset caused by the ultrasound transducer. Therefore, we either used 100% MSO (n = 9) or 120% of rMT (n = 3) during the experiment. The mean percentage of maximum stimulator output was 94.5 ± 10.5%.

The ultrasound transducer was affixed to the center of the TMS coil using the same custom-made 3D-printed clamp as Experiments I & II (***Figure 12B***; DOI: 10.5281/zenodo.6517599). To administer stimulation at high temporal precision, both TUS and TMS were externally triggered via a bossdevice (sync2brain, Tübingen, Germany) using the BEST Toolbox (Hassan et al., 2022), where TMS was consistently applied 10 ms prior to the offset of ultrasound (i.e., following 390 ms of TUS). We tracked and maintained the position of TMS, and by extension TUS, using online neuronavigation in the same manner as described for Experiments I & II.

Electromyography

Muscular activity in the APB was recorded via EMG with surface adhesive electrodes using a belly-tendon montage with the reference electrode placed on the first distal inter-phalangeal joint. The EMG signal was amplified with a gain of 10, low pass filtered at 1250 Hz, and digitally sampled at 5 kHz (Bittium NeurOne Tesla System, Bittium Biosignals Ltd., Finland). The BEST Toolbox controlled data acquisition and saved data for offline analysis (Hassan et al., 2022).

Experimental conditions and procedures

We investigated the role of TUS audibility on motor excitability by administering TUS to an inactive control site – the white matter ventromedial to the hand motor area (***Figure 15A***). In doing so, TUS is applied over a homologous region of the scalp and skull as stimulation of the hand motor area, but without a strong likelihood of direct neuromodulatory effects, allowing us to closely replicate the auditory confound associated with on-target stimulation while simultaneously isolating its effects.

Here, we probed whether the varying volume of the auditory confound at different stimulation intensities might itself impact motor cortical excitability. To this end, we applied stimulation at 4.34, 8.69, and 10.52 W/cm^2 I_{sppa}. We further examined the effects of TUS audibility by applying stimulation both with and without a continuous auditory masking stimulus (***Figure 15B***). This masking stimulus was presented through wired bone-conducting headphones (LBYSK Wired Bone Conduction Headphones) to mimic the auditory confound's mode of entry (Braun et al., 2020). The mask consisted of a 1 kHz square wave with additional white noise added, where the volume and signal-to-noise ratio were increased until the participant could no longer hear TUS, or until the volume became uncomfortable.

We administered conditions in a single-blind inter-subject randomized blocked design. Two blocks were measured per condition, each including 30 TMS-only trials and 30 TUS-TMS trials. TMS-only trials were included in each block to capture any drift in baseline excitability throughout the experiment. TMS-only and TUS-TMS trials were applied in random order within each block, with an inter-trial interval of 5 ± 1 seconds. During blocks with auditory masking, the mask was played continuously throughout the block. Following each block, participants were asked whether they could hear TUS (yes/no/uncertain).

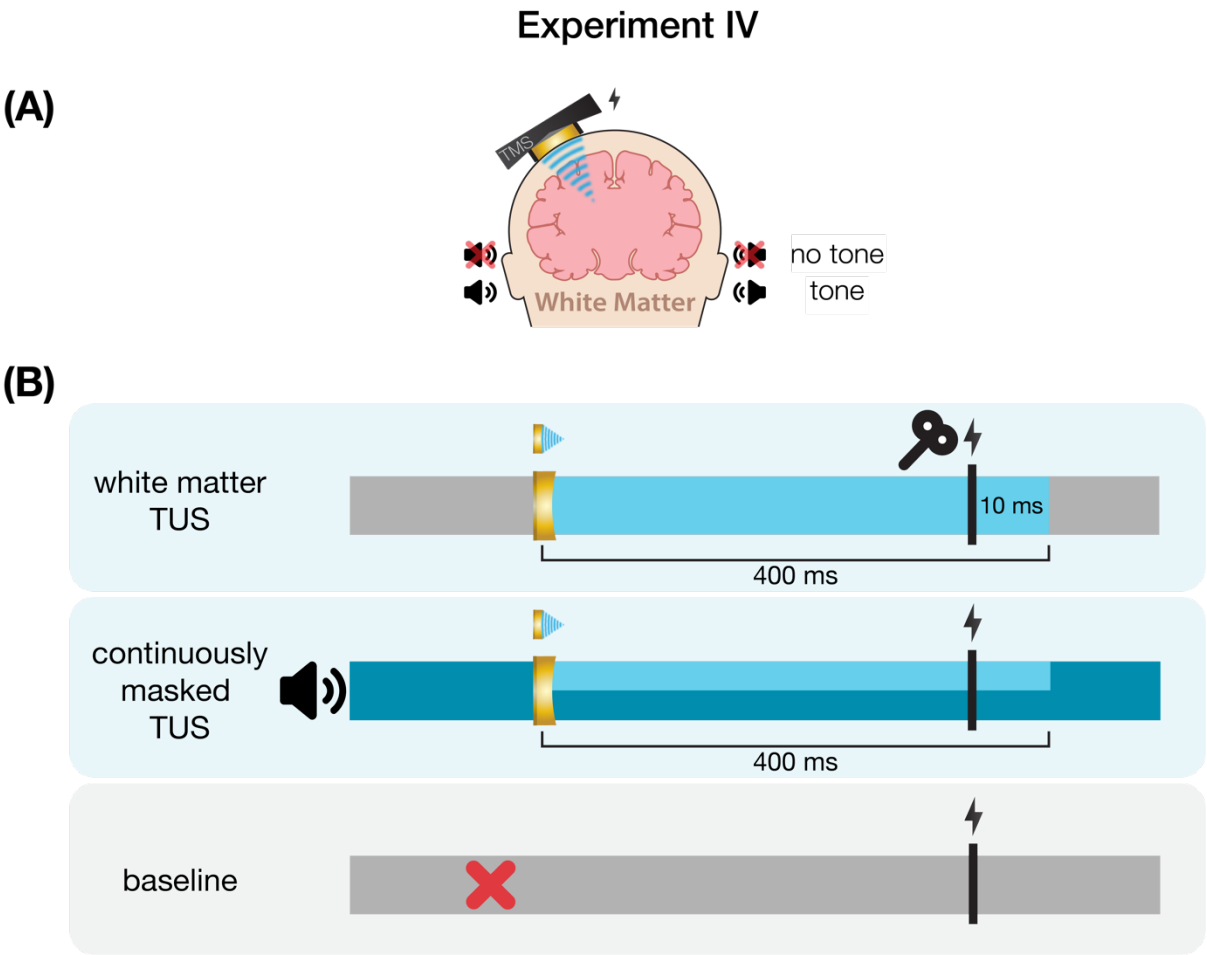

Figure 15. Conditions and timing of Experiment IV. (A) Inactive control stimulation of white matter ventromedial to the left-hemispheric hand motor area. **(B)** White matter TUS was administered for 400 ms, with TMS applied 10 ms prior to TUS-offset. In the masked condition, an auditory stimulus was played continuously throughout the entire block.

Analysis

Data preprocessing and LMMs were conducted using largely identical conventions as Experiments I and II, with the following exception. Given the large number of baseline trials (50% of total), direct comparisons between auditory masking and stimulation intensity (i.e., auditory confound volume) were conducted with baseline corrected MEP amplitude as the dependent variable. Direct comparisons to baseline were conducted with square root corrected MEP amplitude as the dependent variable as in Experiments I and II.

Competing interests

Umair Hassan is the head of software development at sync2brain GmbH, where the bossdevice used in Experiment IV was developed. All other authors declare that no competing interests exist.

Acknowledgements

Experiments I & II were supported by the Dutch Research Council (NWO), awarding VIDI fellowships to L.V. (18919) and H.E.M.d.O. (452-17-016), and the Topsector programme Holland High Tech (HiTMaT-38H3). We thank Brittany van Beek for assistance with data acquisition and administration, Sarmad Peymaei for contributions to technical piloting, Norbert Hermesdorf for developing the 3D-printed TUS-TMS clamp, and Gerard van Oijen and Pascal de Water for their technical support. Experiment III was funded by the Canadian Institutes of Health Research (FDN 154292, ENG 173742) and the Natural Science and Engineering Research Council of Canada (RGPIN-2020-04176, RTI-2020-0024). Experiment IV and T.N. were supported by a grant from the Boehringer Ingelheim Foundation to T.O.B.

Data availability

Data and code required to achieve the reported results will be made available for all four experiments pending peer review.

Additional information

Author contributions

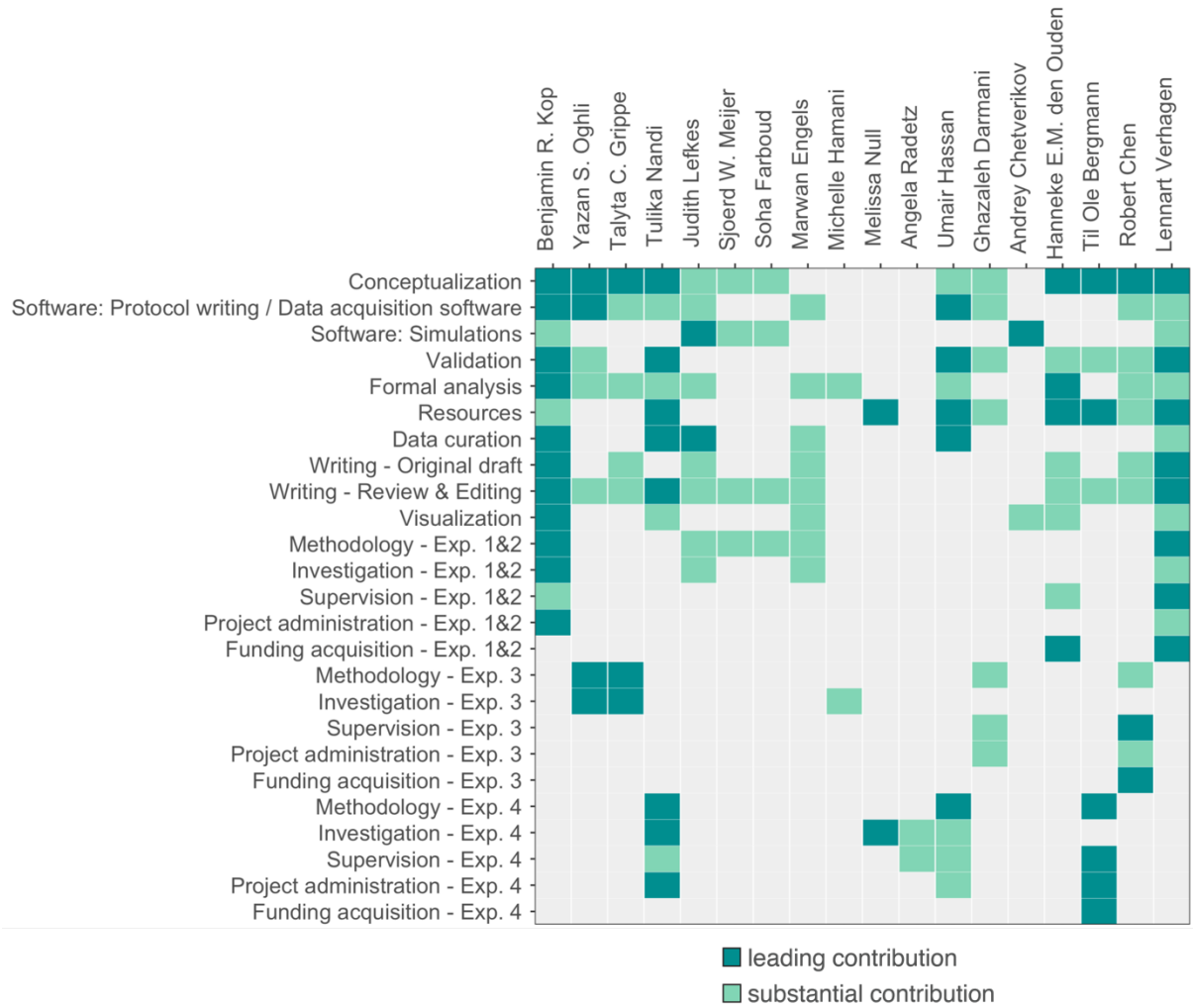

Figure 16. Contribution diagram. This diagram depicts the involvement of each author using the CRediT taxonomy (Brand et al., 2015) and categorizes their contributions according to three levels represented by color: 'none' (gray), 'substantial contribution' (light green), 'leading contribution' (dark green).

Author ORCIDs

Author	ORCID
Benjamin R. Kop	https://orcid.org/0000-0001-7817-5845
Yazan Shamli Oghli	https://orcid.org/0000-0002-9206-6714
Talyta C. Grippe	https://orcid.org/0000-0003-3126-8002
Tulika Nandi	https://orcid.org/0000-0001-8161-3770
Judith Lefkes	https://orcid.org/0000-0003-0813-4049
Sjoerd W. Meijer	https://orcid.org/0000-0003-0698-4525
Soha Farboud	https://orcid.org/0000-0003-2774-3907
Marwan Engels	https://orcid.org/0000-0002-2326-3730
Michelle Hamani	*NA*

Melissa Null	https://orcid.org/0000-0002-4147-7214
Angela Radetz	https://orcid.org/0000-0003-2622-3221
Umair Hassan	https://orcid.org/0000-0001-8245-0061
Ghazaleh Darmani	https://orcid.org/0000-0002-4073-1911
Andrey Chetverikov	https://orcid.org/0000-0003-2767-6310
Hanneke E.M. den Ouden	https://orcid.org/0000-0001-7039-5130
Til Ole Bergmann	https://orcid.org/0000-0002-2282-6618
Robert Chen	https://orcid.org/0000-0002-8371-8629
Lennart Verhagen	https://orcid.org/0000-0003-3207-7929

Appendix

Simulation outputs

Supplementary Table 1. Simulation outputs for Experiments I and II.

	n	I_{sppa} (W/cm^2)	Intracranial I_{sppa}[1] (W/cm^2)	MI[1]	ΔT[1] (°C)
Experiment I	9	32.5	9.57 ± 1.56	0.78 ± 0.06	0.34 ± 0.13
		65	19.13 ± 3.13	1.10 ± 0.09	0.68 ± 0.27
Experiment II	27	6.35	1.75 ± 0.48	0.47 ± 0.06	0.07 ± 0.03
		19.06	5.26 ± 1.43	0.81 ± 0.11	0.20 ± 0.09

[1]mean±SD

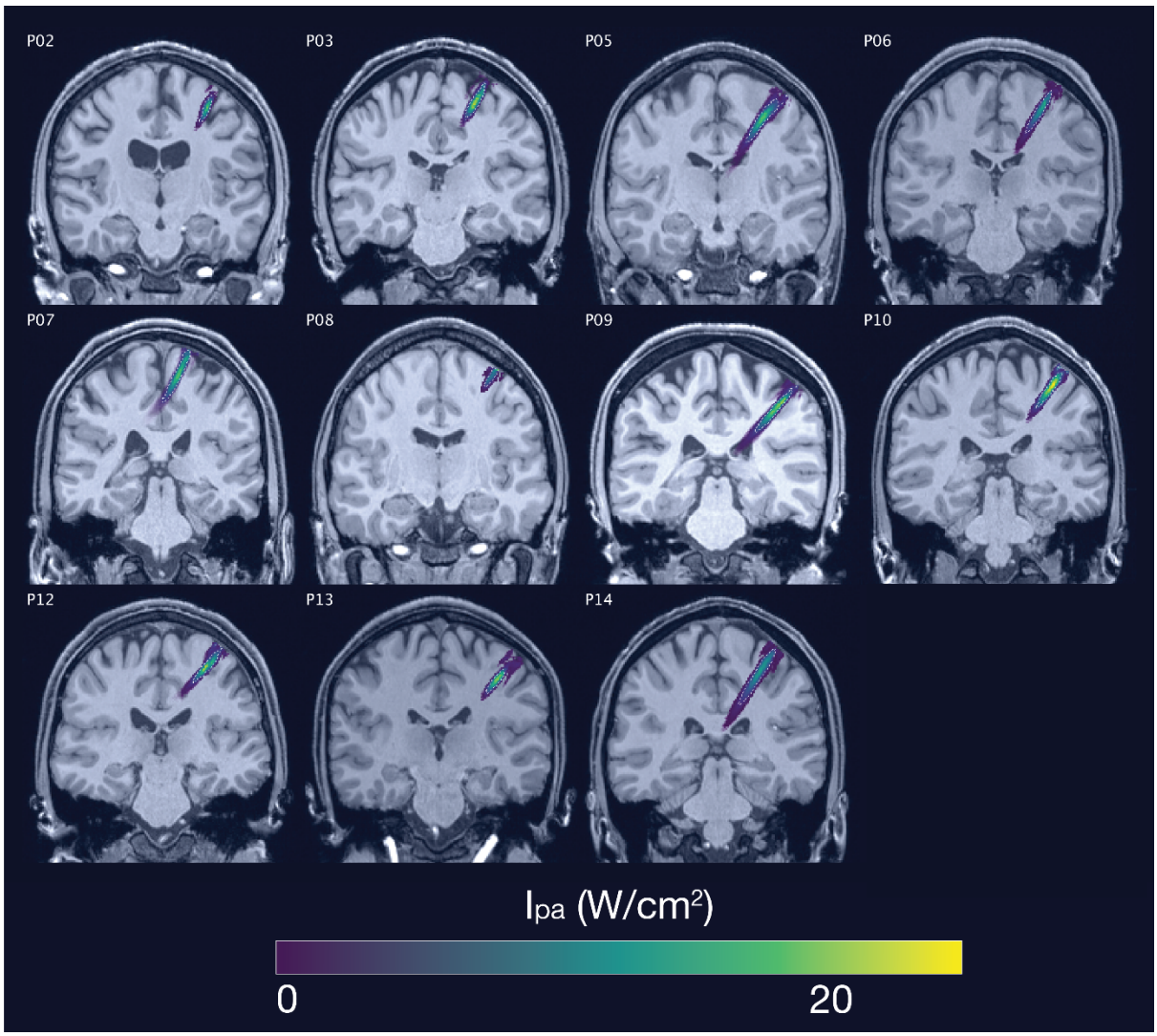

Supplementary Figure 1. Acoustic simulations. Individual simulations for Experiment I of acoustic wave propagation at 65 W/cm^2 free-water stimulation intensity. Simulated pulse-average intensities above 0.15 W/cm^2 are depicted. The FWHM of the pressure is indicated by the dashed white line.

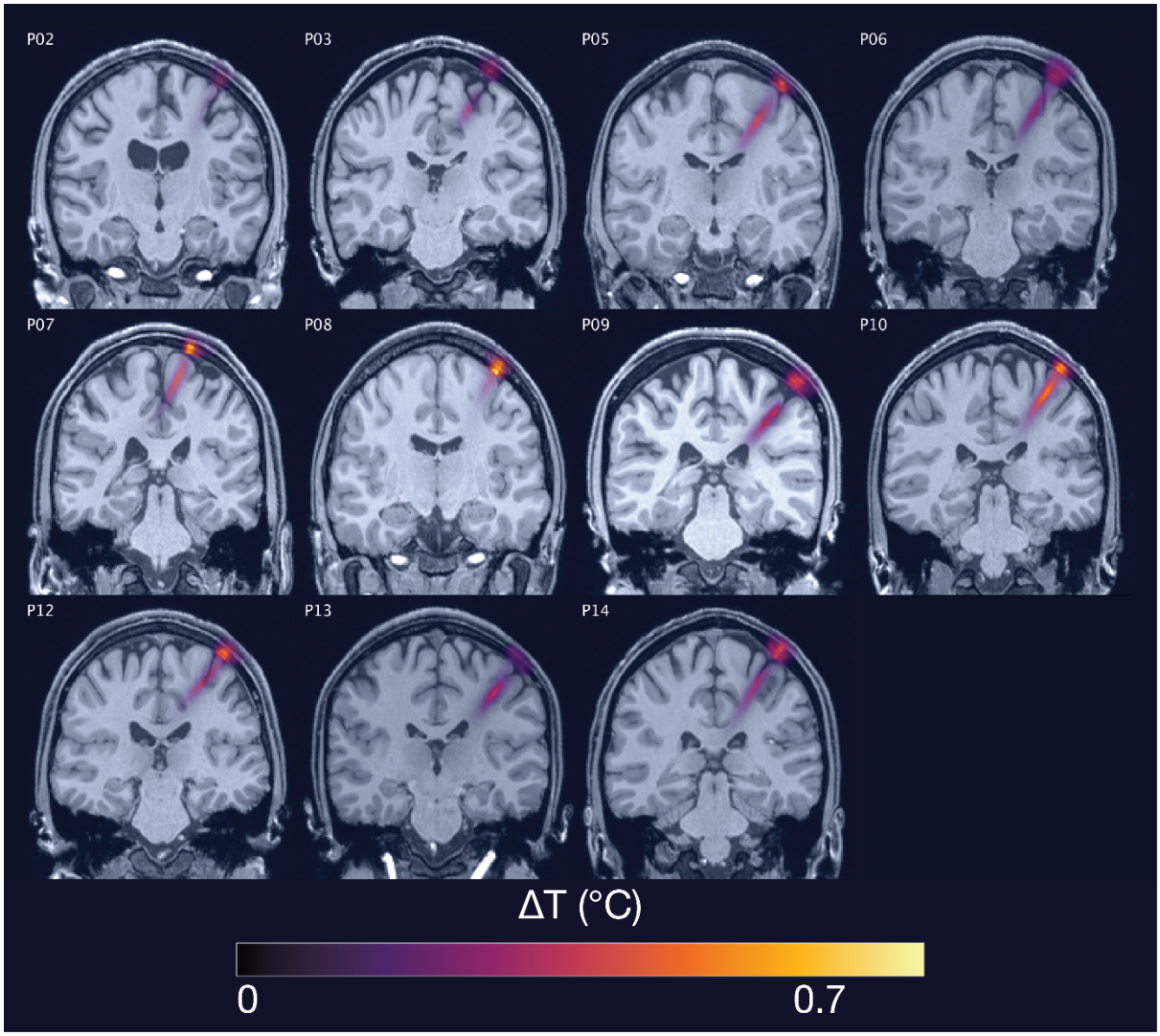

Supplementary Figure 2. Thermal simulations. Individual simulations for Experiment I of thermal rise at 65 W/cm^2 free-water stimulation intensity.

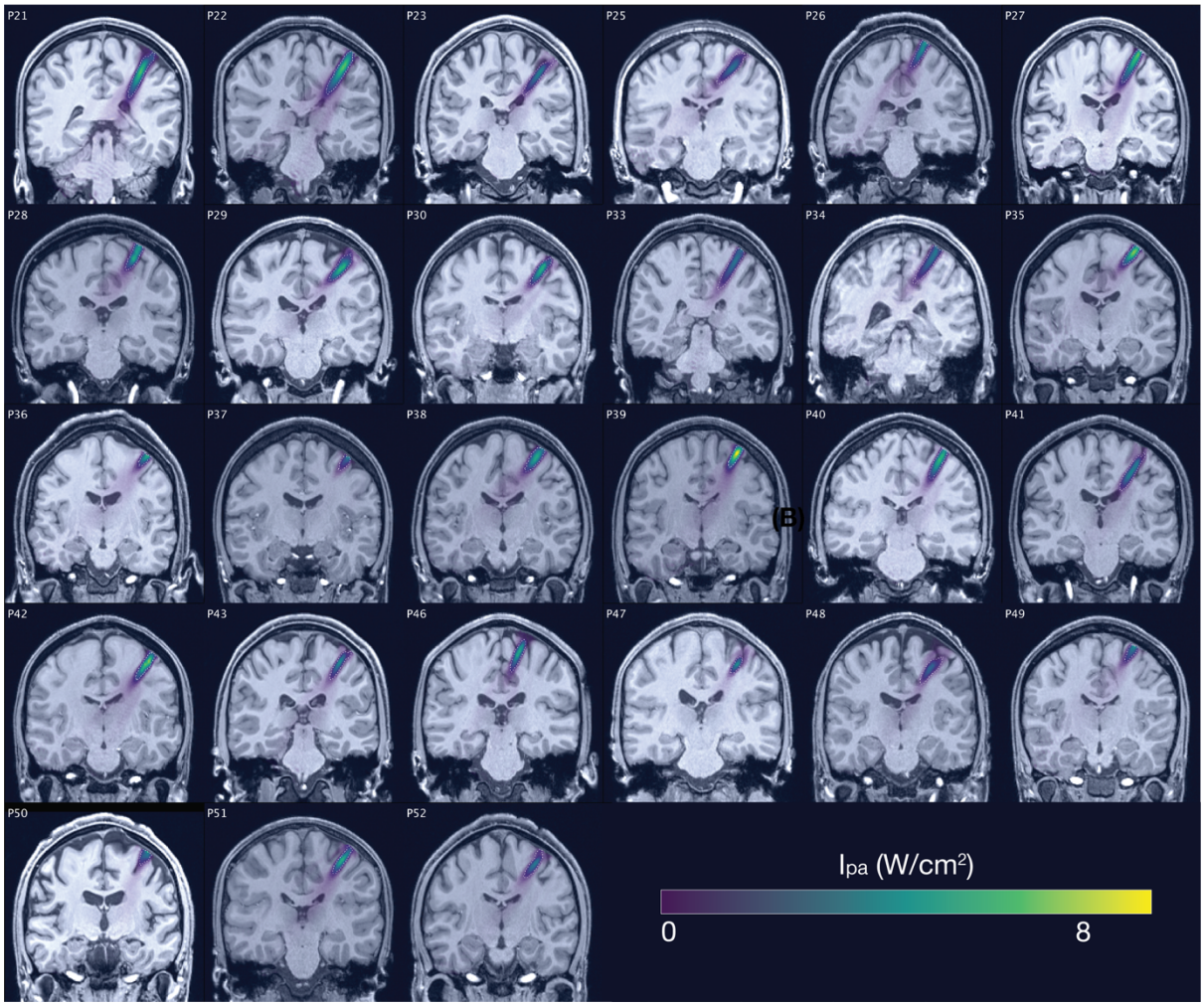

Supplementary Figure 3. Acoustic simulations. Individual simulations for Experiment II of acoustic wave propagation at 19.05 W/cm^2 free-water stimulation intensity. Simulated pulse-average intensities above 0.15 W/cm^2 are depicted. The FWHM of the pressure is indicated by the dashed white line.

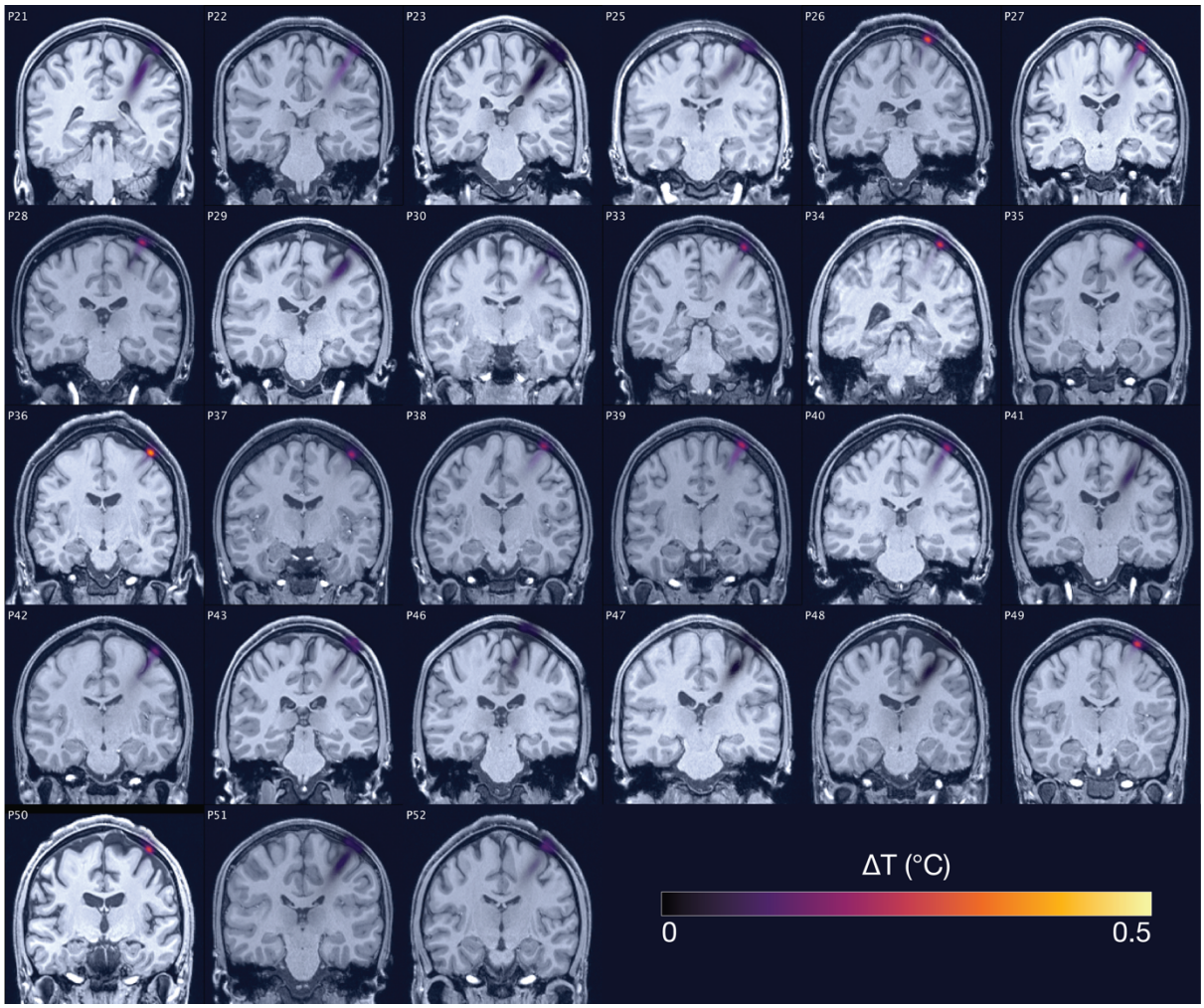

Supplementary Figure 4. Thermal simulations. Individual simulations for Experiment II of thermal rise at 19.05 W/cm^2 free-water stimulation intensity.

Experiment III: TMS intensity required to evoke a ~1 mV MEP

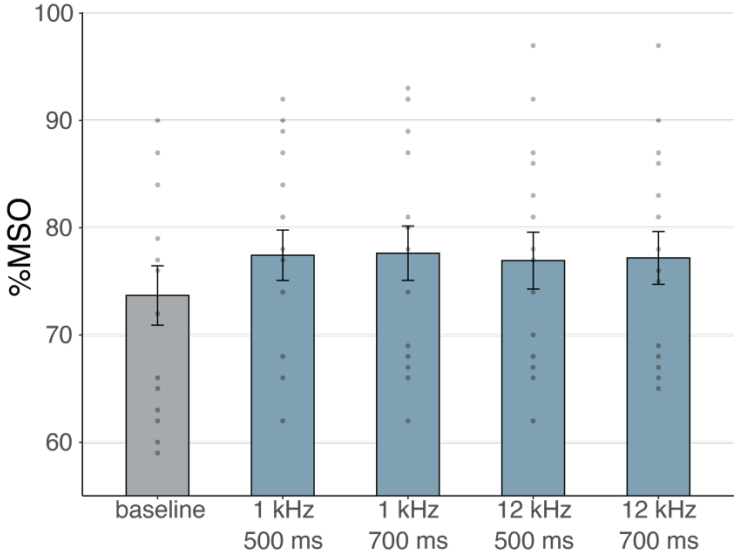

Supplementary Figure 6. TMS intensity. The percentage maximum stimulator output (%MSO) required to evoke a ~1 mV MEP during baseline (Part I) and the four sound-sham conditions (Part II).

References

Ai, L., Bansal, P., Mueller, J. K., & Legon, W. (2018). Effects of transcranial focused ultrasound on human primary motor cortex using 7T fMRI: A pilot study. *BMC Neuroscience*, *19*(1), 56. https://doi.org/10.1186/s12868-018-0456-6

Ai, L., Mueller, J. K., Grant, A., Eryaman, Y., & Legon, W. (2016). Transcranial focused ultrasound for BOLD fMRI signal modulation in humans. *2016 38th Annual International Conference of the IEEE Engineering in Medicine and Biology Society (EMBC)*, 1758–1761. https://doi.org/10.1109/EMBC.2016.7591057

Airan, R. D., & Butts Pauly, K. (2018). Hearing out Ultrasound Neuromodulation. *Neuron*, *98*(5), 875–877. https://doi.org/10.1016/j.neuron.2018.05.031

Aubry, J.-F., Bates, O., Boehm, C., Pauly, K. B., Christensen, D., Cueto, C., Gelat, P., Guasch, L., Jaros, J., Jing, Y., Jones, R., Li, N., Marty, P., Montanaro, H., Neufeld, E., Pichardo, S., Pinton, G., Pulkkinen, A., Stanziola, A., … Wout, E. van ’t. (2022). *Benchmark problems for transcranial ultrasound simulation: Intercomparison of compressional wave models*. https://doi.org/10.48550/ARXIV.2202.04552

Barr, D. J., Levy, R., Scheepers, C., & Tily, H. J. (2013). Random effects structure for confirmatory hypothesis testing: Keep it maximal. *Journal of Memory and Language*, *68*(3), 255–278. https://doi.org/10.1016/j.jml.2012.11.001

Bates, D., Mächler, M., Bolker, B., & Walker, S. (2015). Fitting Linear Mixed-Effects Models Using lme4. *Journal of Statistical Software*, *67*(1). https://doi.org/10.18637/jss.v067.i01

Bergmann, T. O., & Hartwigsen, G. (2021). Inferring Causality from Noninvasive Brain Stimulation in Cognitive Neuroscience. *Journal of Cognitive Neuroscience*, *33*(2), 195–225. https://doi.org/10.1162/jocn_a_01591

Bestmann, S., & Walsh, V. (2017). Transcranial electrical stimulation. *Current Biology*, *27*(23), R1258–R1262. https://doi.org/10.1016/j.cub.2017.11.001

Biabani, M., Farrell, M., Zoghi, M., Egan, G., & Jaberzadeh, S. (2018). The minimal number of TMS trials required for the reliable assessment of corticospinal excitability, short interval intracortical inhibition, and intracortical facilitation. *Neuroscience Letters*, *674*, 94–100. https://doi.org/10.1016/j.neulet.2018.03.026

Brand, A., Allen, L., Altman, M., Hlava, M., & Scott, J. (2015). Beyond authorship: Attribution, contribution, collaboration, and credit. *Learned Publishing*, *28*(2), 151–155. https://doi.org/10.1087/20150211

Braun, V., Blackmore, J., Cleveland, R. O., & Butler, C. R. (2020). Transcranial ultrasound stimulation in humans is associated with an auditory confound that can be effectively masked. *Brain Stimulation*, *13*(6), 1527–1534. https://doi.org/10.1016/j.brs.2020.08.014

Cain, J. A., Visagan, S., Johnson, M. A., Crone, J., Blades, R., Spivak, N. M., Shattuck, D. W., & Monti, M. M. (2021). Real time and delayed effects of subcortical low intensity focused ultrasound. *Scientific Reports*, *11*(1), 6100. https://doi.org/10.1038/s41598-021-85504-y

Capozio, A., Chakrabarty, S., & Astill, S. (2021). The Effect of Sound and Stimulus Expectation on Transcranial Magnetic Stimulation-Elicited Motor Evoked Potentials. *Brain Topography*, *34*(6), 720–730. https://doi.org/10.1007/s10548-021-00867-9

Conde, V., Tomasevic, L., Akopian, I., Stanek, K., Saturnino, G. B., Thielscher, A., Bergmann, T. O., & Siebner, H. R. (2019). The non-transcranial TMS-evoked potential is an inherent source of ambiguity in TMS-EEG studies. *NeuroImage*, *185*, 300–312. https://doi.org/10.1016/j.neuroimage.2018.10.052

Darmani, G., Bergmann, T. O., Butts Pauly, K., Caskey, C. F., de Lecea, L., Fomenko, A., Fouragnan, E., Legon, W., Murphy, K. R., Nandi, T., Phipps, M. A., Pinton, G., Ramezanpour, H., Sallet, J., Yaakub, S. N., Yoo, S. S., & Chen, R. (2022). Non-invasive transcranial ultrasound stimulation for neuromodulation. *Clinical Neurophysiology*, *135*, 51–73. https://doi.org/10.1016/j.clinph.2021.12.010

Duecker, F., de Graaf, T. A., Jacobs, C., & Sack, A. T. (2013). Time- and Task-Dependent Non-Neural Effects of Real and Sham TMS. *PLoS ONE*, *8*(9), e73813. https://doi.org/10.1371/journal.pone.0073813

El Hady, A., & Machta, B. B. (2015). Mechanical surface waves accompany action potential propagation. *Nature Communications*, *6*(1), Article 1. https://doi.org/10.1038/ncomms7697

Felix, C., Folloni, D., Chen, H., Sallet, J., & Jerusalem, A. (2022). White matter tract transcranial ultrasound stimulation, a computational study. *Computers in Biology and Medicine*, *140*, 105094. https://doi.org/10.1016/j.compbiomed.2021.105094

Fisher, R. J., Sharott, A., K hn, A. A., & Brown, P. (2004). Effects of combined cortical and acoustic stimuli on muscle activity. *Experimental Brain Research*, *157*(1), 1–9. https://doi.org/10.1007/s00221-003-1809-6

Folloni, D., Verhagen, L., Mars, R. B., Fouragnan, E., Constans, C., Aubry, J.-F., Rushworth, M. F. S., & Sallet, J. (2019). Manipulation of Subcortical and Deep Cortical Activity in the Primate Brain Using Transcranial Focused Ultrasound Stimulation. *Neuron*, *101*(6), 1109-1116.e5. https://doi.org/10.1016/j.neuron.2019.01.019

Fomenko, A., Chen, K.-H. S., Nankoo, J.-F., Saravanamuttu, J., Wang, Y., El-Baba, M., Xia, X., Seerala, S. S., Hynynen, K., Lozano, A. M., & Chen, R. (2020). Systematic examination of low-intensity ultrasound parameters on human motor cortex excitability and behavior. *ELife*, *9*, e54497. https://doi.org/10.7554/eLife.54497

Ford, J. M., Gray, M., Faustman, W. O., Roach, B. J., & Mathalon, D. H. (2007). Dissecting corollary discharge dysfunction in schizophrenia. *Psychophysiology*, *44*(4), 522–529. https://doi.org/10.1111/j.1469-8986.2007.00533.x

Furubayashi, T., Ugawa, Y., Terao, Y., Hanajima, R., Sakai, K., Machii, K., Mochizuki, H., Shiio, Y., Uesugi, H., Enomoto, H., & Kanazawa, I. (2000). The human hand motor area is transiently suppressed by an unexpected auditory stimulus. *Clinical Neurophysiology*, *111*(1), 178–183. https://doi.org/10.1016/S1388-2457(99)00200-X

Goldsworthy, M. R., Hordacre, B., & Ridding, M. C. (2016). Minimum number of trials required for within- and between-session reliability of TMS measures of corticospinal excitability. *Neuroscience*, *320*, 205–209. https://doi.org/10.1016/j.neuroscience.2016.02.012

Guo, H., Hamilton, M., Offutt, S. J., Gloeckner, C. D., Li, T., Kim, Y., Legon, W., Alford, J. K., & Lim, H. H. (2018). Ultrasound Produces Extensive Brain Activation via a Cochlear Pathway. *Neuron*, *98*(5), 1020-1030.e4. https://doi.org/10.1016/j.neuron.2018.04.036

Hamani, C., Mayberg, H., Stone, S., Laxton, A., Haber, S., & Lozano, A. M. (2011). The Subcallosal Cingulate Gyrus in the Context of Major Depression. *Biological Psychiatry*, *69*(4), 301–308. https://doi.org/10.1016/j.biopsych.2010.09.034

Hassan, U., Pillen, S., Zrenner, C., & Bergmann, T. O. (2022). The Brain Electrophysiological recording & STimulation (BEST) toolbox. *Brain Stimulation*, *15*(1), 109–115. https://doi.org/10.1016/j.brs.2021.11.017

Heimburg, T., & Jackson, A. D. (2005). On soliton propagation in biomembranes and nerves. *Proceedings of the National Academy of Sciences*, *102*(28), 9790–9795. https://doi.org/10.1073/pnas.0503823102

Ilic, T. V., Pötter-Nerger, M., Holler, I., Siebner, H. R., Ilic, N. V., Deuschl, G., & Volkmann, J. (2011). Startle Stimuli Exert Opposite Effects on Human Cortical and Spinal Motor System Excitability in Leg Muscles. *Physiological Research*, S101–S106. https://doi.org/10.33549/physiolres.932182

IT'IS Foundation. (2022). *Tissue Properties Database V4.1* [..Db, .xls, .txt, .pdf]. IT'IS Foundation. https://doi.org/10.13099/VIP21000-04-1

Johnstone, A., Nandi, T., Martin, E., Bestmann, S., Stagg, C., & Treeby, B. (2021). A range of pulses commonly used for human transcranial ultrasound stimulation are clearly audible. *Brain Stimulation*, *14*(5), 1353–1355. https://doi.org/10.1016/j.brs.2021.08.015

Kubanek, J., Shukla, P., Das, A., Baccus, S. A., & Goodman, M. B. (2018). Ultrasound Elicits Behavioral Responses through Mechanical Effects on Neurons and Ion Channels in a Simple Nervous

System. *The Journal of Neuroscience*, *38*(12), 3081–3091. https://doi.org/10.1523/JNEUROSCI.1458-17.2018

K?hn, AndreaA., Sharott, A., Trottenberg, T., Kupsch, A., & Brown, P. (2004). Motor cortex inhibition induced by acoustic stimulation. *Experimental Brain Research*, *158*(1). https://doi.org/10.1007/s00221-004-1883-4

Lee, W., Kim, H.-C., Jung, Y., Chung, Y. A., Song, I.-U., Lee, J.-H., & Yoo, S.-S. (2016). Transcranial focused ultrasound stimulation of human primary visual cortex. *Scientific Reports*, *6*(1), 34026. https://doi.org/10.1038/srep34026

Legon, W., Ai, L., Bansal, P., & Mueller, J. K. (2018). Neuromodulation with single-element transcranial focused ultrasound in human thalamus. *Human Brain Mapping*, *39*(5), 1995–2006. https://doi.org/10.1002/hbm.23981

Legon, W., Bansal, P., Tyshynsky, R., Ai, L., & Mueller, J. K. (2018). Transcranial focused ultrasound neuromodulation of the human primary motor cortex. *Scientific Reports*, *8*. https://doi.org/10.1038/s41598-018-28320-1

Lemaire, T., Neufeld, E., Kuster, N., & Micera, S. (2019). Understanding ultrasound neuromodulation using a computationally efficient and interpretable model of intramembrane cavitation. *Journal of Neural Engineering*, *16*(4), 046007. https://doi.org/10.1088/1741-2552/ab1685

Liu, C., Yu, K., Niu, X., & He, B. (2021). Transcranial Focused Ultrasound Enhances Sensory Discrimination Capability through Somatosensory Cortical Excitation. *Ultrasound in Medicine & Biology*, *47*(5), 1356–1366. https://doi.org/10.1016/j.ultrasmedbio.2021.01.025

Lozano, A. M., Mayberg, H. S., Giacobbe, P., Hamani, C., Craddock, R. C., & Kennedy, S. H. (2008). Subcallosal Cingulate Gyrus Deep Brain Stimulation for Treatment-Resistant Depression. *Biological Psychiatry*, *64*(6), 461–467. https://doi.org/10.1016/j.biopsych.2008.05.034

Mayberg, H. S., Lozano, A. M., Voon, V., McNeely, H. E., Seminowicz, D., Hamani, C., Schwalb, J. M., & Kennedy, S. H. (2005). Deep Brain Stimulation for Treatment-Resistant Depression. *Neuron*, *45*(5), 651–660. https://doi.org/10.1016/j.neuron.2005.02.014

Menz, M. D., Oralkan, O., Khuri-Yakub, P. T., & Baccus, S. A. (2013). Precise neural stimulation in the retina using focused ultrasound. *The Journal of Neuroscience: The Official Journal of the Society for Neuroscience*, *33*(10), 4550–4560. https://doi.org/10.1523/JNEUROSCI.3521-12.2013

Mohammadjavadi, M., Ye, P. P., Xia, A., Brown, J., Popelka, G., & Pauly, K. B. (2019). Elimination of peripheral auditory pathway activation does not affect motor responses from ultrasound neuromodulation. *Brain Stimulation*, *12*(4), 901–910. https://doi.org/10.1016/j.brs.2019.03.005

Monti, M. M., Schnakers, C., Korb, A. S., Bystritsky, A., & Vespa, P. M. (2016). Non-Invasive Ultrasonic Thalamic Stimulation in Disorders of Consciousness after Severe Brain Injury: A First-in-Man Report. *Brain Stimulation*, *9*(6), 940–941. https://doi.org/10.1016/j.brs.2016.07.008

Murphy, K. R., Farrell, J. S., Gomez, J. L., Stedman, Q. G., Li, N., Leung, S. A., Good, C. H., Qiu, Z., Firouzi, K., Butts Pauly, K., Khuri-Yakub, B. P. T., Michaelides, M., Soltesz, I., & de Lecea, L. (2022). A tool for monitoring cell type–specific focused ultrasound neuromodulation and control of chronic epilepsy. *Proceedings of the National Academy of Sciences*, *119*(46), e2206828119. https://doi.org/10.1073/pnas.2206828119

Nakajima, K., Osada, T., Ogawa, A., Tanaka, M., Oka, S., Kamagata, K., Aoki, S., Oshima, Y., Tanaka, S., & Konishi, S. (2022). A causal role of anterior prefrontal-putamen circuit for response inhibition revealed by transcranial ultrasound stimulation in humans. *Cell Reports*, *40*(7), 111197. https://doi.org/10.1016/j.celrep.2022.111197

Osada, T., Nakajima, K., Ogawa, A., Oka, S., Kamagata, K., Aoki, S., Oshima, Y., Tanaka, S., & Konishi, S. (2022). Distributions of cortical depth of the index finger region in the M1: A representative depth parameter for transcranial ultrasound stimulation. *Brain Stimulation*, *15*(6), 1348–1350. https://doi.org/10.1016/j.brs.2022.09.012

O'Shea, J., & Walsh, V. (2007). Transcranial magnetic stimulation. *Current Biology*, *17*(6), R196–R199. https://doi.org/10.1016/j.cub.2007.01.030

Plaksin, M., Shoham, S., & Kimmel, E. (2014). Intramembrane Cavitation as a Predictive Bio-Piezoelectric Mechanism for Ultrasonic Brain Stimulation. *Physical Review X*, *4*(1), 011004. https://doi.org/10.1103/PhysRevX.4.011004

Polanía, R., Nitsche, M. A., & Ruff, C. C. (2018). Studying and modifying brain function with non-invasive brain stimulation. *Nature Neuroscience*, *21*(2), 174–187. https://doi.org/10.1038/s41593-017-0054-4

Prieto, M. L., Oralkan, Ö., Khuri-Yakub, B. T., & Maduke, M. C. (2013). Dynamic Response of Model Lipid Membranes to Ultrasonic Radiation Force. *PLOS ONE*, *8*(10), e77115. https://doi.org/10.1371/journal.pone.0077115

Salahshoor, H., Shapiro, M. G., & Ortiz, M. (2020). Transcranial focused ultrasound generates skull-conducted shear waves: Computational model and implications for neuromodulation. *Applied Physics Letters*, *117*(3), 033702. https://doi.org/10.1063/5.0011837

Sato, T., Shapiro, M. G., & Tsao, D. Y. (2018). Ultrasonic Neuromodulation Causes Widespread Cortical Activation via an Indirect Auditory Mechanism. *Neuron*, *98*(5), 1031-1041.e5. https://doi.org/10.1016/j.neuron.2018.05.009

Schmahmann, J. D., & Pandya, D. N. (2006). *Fiber Pathways of the Brain*. Oxford University Press. https://doi.org/10.1093/acprof:oso/9780195104233.001.0001

Siebner, H. R., Funke, K., Aberra, A. S., Antal, A., Bestmann, S., Chen, R., Classen, J., Davare, M., Di Lazzaro, V., Fox, P. T., Hallett, M., Karabanov, A. N., Kesselheim, J., Beck, M. M., Koch, G., Liebetanz, D., Meunier, S., Miniussi, C., Paulus, W., … Ugawa, Y. (2022). Transcranial magnetic stimulation of the brain: What is stimulated? – A consensus and critical position paper. *Clinical Neurophysiology*, *140*, 59–97. https://doi.org/10.1016/j.clinph.2022.04.022

Stenfelt, S., & Håkansson, B. (2002). Air versus bone conduction: An equal loudness investigation. *Hearing Research*, *167*(1–2), 1–12. https://doi.org/10.1016/S0378-5955(01)00407-5

Thielscher, A., Antunes, A., & Saturnino, G. B. (2015). Field modeling for transcranial magnetic stimulation: A useful tool to understand the physiological effects of TMS? *2015 37th Annual*

International Conference of the IEEE Engineering in Medicine and Biology Society (EMBC), 222–225. https://doi.org/10.1109/EMBC.2015.7318340

Tran, D. M. D., McNair, N. A., Harris, J. A., & Livesey, E. J. (2021a). Expected TMS excites the motor system less effectively than unexpected stimulation. *NeuroImage*, *226*, 117541. https://doi.org/10.1016/j.neuroimage.2020.117541

Tran, D. M. D., McNair, N. A., Harris, J. A., & Livesey, E. J. (2021b). Expected TMS excites the motor system less effectively than unexpected stimulation. *NeuroImage*, *226*, 117541. https://doi.org/10.1016/j.neuroimage.2020.117541

Treeby, B. E., & Cox, B. T. (2010). k-Wave: MATLAB toolbox for the simulation and reconstruction of photoacoustic wave fields. *Journal of Biomedical Optics*, *15*(2), 021314. https://doi.org/10.1117/1.3360308

Tyler, W. J., Lani, S. W., & Hwang, G. M. (2018). Ultrasonic modulation of neural circuit activity. *Current Opinion in Neurobiology*, *50*, 222–231. https://doi.org/10.1016/j.conb.2018.04.011

Tyler, W. J., Tufail, Y., Finsterwald, M., Tauchmann, M. L., Olson, E. J., & Majestic, C. (2008). Remote Excitation of Neuronal Circuits Using Low-Intensity, Low-Frequency Ultrasound. *PLoS ONE*, *3*(10), e3511. https://doi.org/10.1371/journal.pone.0003511

Verhagen, L., Gallea, C., Folloni, D., Constans, C., Jensen, D. E., Ahnine, H., Roumazeilles, L., Santin, M., Ahmed, B., Lehericy, S., Klein-Flügge, M. C., Krug, K., Mars, R. B., Rushworth, M. F., Pouget, P., Aubry, J.-F., & Sallet, J. (2019). Offline impact of transcranial focused ultrasound on cortical activation in primates. *ELife*, *8*, e40541. https://doi.org/10.7554/eLife.40541

Weinreb, E., & Moses, E. (2022). Mechanistic insights into ultrasonic neurostimulation of disconnected neurons using single short pulses. *Brain Stimulation*, *15*(3), 769–779. https://doi.org/10.1016/j.brs.2022.05.004

Wessel, J. R., & Aron, A. R. (2013). Unexpected Events Induce Motor Slowing via a Brain Mechanism for Action-Stopping with Global Suppressive Effects. *Journal of Neuroscience*, *33*(47), 18481–18491. https://doi.org/10.1523/JNEUROSCI.3456-13.2013

Xia, X., Fomenko, A., Nankoo, J.-F., Zeng, K., Wang, Y., Zhang, J., Lozano, A. M., & Chen, R. (2021). Time course of the effects of low-intensity transcranial ultrasound on the excitability of ipsilateral and contralateral human primary motor cortex. *NeuroImage*, *243*, 118557. https://doi.org/10.1016/j.neuroimage.2021.118557

Yoo, S., Mittelstein, D. R., Hurt, R. C., Lacroix, J., & Shapiro, M. G. (2022). Focused ultrasound excites cortical neurons via mechanosensitive calcium accumulation and ion channel amplification. *Nature Communications*, *13*(1), 493. https://doi.org/10.1038/s41467-022-28040-1

Zeng, K., Darmani, G., Fomenko, A., Xia, X., Tran, S., Nankoo, J., Shamli Oghli, Y., Wang, Y., Lozano, A. M., & Chen, R. (2022). Induction of Human Motor Cortex Plasticity by Theta Burst Transcranial Ultrasound Stimulation. *Annals of Neurology*, ana.26294. https://doi.org/10.1002/ana.26294